

Investigating lipopolysaccharide-induced inflammation in Sprague-Dawley rats on liver function with specific focus on coagulation factor production

By

Karabo Rathebe

Student number: 11214491

Supervisor: Prof Janette Bester

janette.bester@up.ac.za

Co-supervisor: Dr Sajee Allumoottill

sajee.alummoottill@up.ac.za

Department: Physiology

Degree: MSc in Human Physiology

Abstract

Neurodegenerative diseases, such as Parkinson's disease (PD) and Alzheimer's disease (AD), have long confounded the scientific and medical communities. The extensive research into these diseases, particularly AD has produced several plausible theories on its progression, but this research has so far failed to yield any lasting results in producing an effective treatment of AD. With the increase of the prevalence of AD in an increasingly aging world population, elucidating a model of disease progression that takes into account the neurodegenerative characteristics that are hallmarks of the disease, along with its related metabolic and organ system effects has become a public health priority. Systemic inflammation has become one of the main components of several non-communicable diseases, in particular AD.

In this study, the aim was to investigate an emerging theory of AD pathogenesis that may combine the neurological and metabolic aspects that are often seen in these patients, the gut-liver axis theory. This theory states that the liver is the first organ to come into contact with circulating lipopolysaccharide (LPS), which would cause the kind of low-grade and chronic inflammation that would cause significant long-term damage to the liver, thus resulting in the organ system failure secondary to AD. Therefore, a model of LPS-induced inflammation was studied in adult male Sprague-Dawley rats to determine the effect of the systemically -induced LPS inflammation on the liver with particular focus on coagulation factor production and the possible prevalence of liver damage and fibrosis.

The model was successfully created over a 10-day period, after which the animals were terminated, and the liver tissues collected and processed for use in light-microscopy and transmission electron microscopy (TEM). The levels of coagulation factors, tissue factor (TF) and fibrinogen (FG), were also determined by use of ELISA assays. Behavioural testing was used as a means to confirm the presence of AD-like symptoms in the model induced by the LPS administration.

Due to the low concentration of LPS administered into the animals during the experimental period, the levels of tissue factor and fibrinogen were not significantly higher or changed when compared with the control group. Similarly, the morphological analysis of liver tissue showed that the administration of LPS as designed in this study did not significantly affect the liver tissue. At an

organelle level, it was found that the LPS administration produced a mild to moderate negative effect on the liver, an indication of the initial stages of liver damage due to the exposure of LPS.

In conclusion, the administration of LPS in Sprague-Dawley rats as modelled in this study did not induce the systemic inflammation that would cause significant liver damage and subsequent fibrosis, only producing the initial stages liver damage seen at sub-microscopic level. This however shows that short-term exposure to low levels of LPS will induce changes on a cellular level and that long-term exposure could accumulate to complications that could lead to clinical presentation.

Key words: inflammation, lipopolysaccharide, liver

Table of Contents

Abstract.....	i
Investigating lipopolysaccharide-induced inflammation in Sprague-Dawley rats on liver function with specific focus on coagulation factor production.....	1
Chapter One	9
Introduction	9
Chapter Two	12
Literature Review	12
Chapter Objectives	13
2.1 Alzheimer’s disease: a brief overview	13
2.2 Lipopolysaccharide and Alzheimer’s disease.....	13
2.3 Inflammation and liver function	15
2.3.1 Inflammation and coagulation.....	17
2.4 Hypercoagulability: pathogenesis and consequences.....	21
2.4.1 The hypercoagulable state in Alzheimer’s disease	21
2.4.2 Linking hypercoagulability and liver dysfunction	22
Chapter Three.....	25
3.1 Chapter Objectives	26
3.1.1 Ethical considerations.....	26
3.2 Methods and Materials	27
3.2.1 Materials.....	27
3.2.2 Methods.....	27
3.2.2.1 Implementation of the model.....	27
3.2.2.2 Observations made during the experimental period	30
3.2.2.3 Behavioural studies.....	30
3.2.2.4 Termination.....	32
3.2.2.5 Tissue sample collection	32
3.2.2.6 Statistical Analysis	34
Chapter Four	36
4.1 Chapter Objectives	37
4.1.1 Introduction.....	37
4.2 Methods and Materials	38
4.2.1 Materials.....	38
4.2.2 Methods.....	38
4.2.3 Statistical analysis	38
4.3 Results	39

4.4 Discussion	41
4.5 Conclusion.....	41
5.1 Chapter Objectives	44
5.1.1 Introduction.....	44
5.2 Materials and methods	45
5.2.1 List of reagents and materials used	45
5.2.2 Tissue extraction for light microscopy	46
5.2.3 Paraffin wax embedding with tert- <i>Butyl</i> alcohol.....	46
5.2.4 Haematoxylin & Eosin staining	46
5.2.5 Picrosirius red staining.....	46
5.3 Results	47
5.3.1 Haematoxylin and eosin staining	47
5.3.2 Picrosirius red staining.....	48
5.4 Discussion	50
5.5 Conclusion.....	51
6.1 Objectives.....	53
6.1.1 Introduction.....	53
6.2 Materials and methods	54
6.2.1 List of reagents and materials.....	54
6.2.2 Tissue extraction and fixation with 2.5% glutaraldehyde/formaldehyde.....	55
6.3 Results	55
6.4 Discussion	63
6.5 Conclusion.....	64
7.1 Chapter Objectives	66
7.1.1 Introduction.....	66
7.2 Methods and materials	67
7.2.1 List of reagents and materials.....	67
7.2.2 Tissue extraction for ELISA testing	67
7.2.3 Detection of tissue factor and fibrinogen levels in liver tissue.....	67
7.3 Statistical analysis	68
7.4 Results.....	68
7.5 Discussion.....	70
7.6 Conclusion	70
Chapter Eight	71
Appendices.....

Appendix A: Ethics documentation

Appendix B: Turnitin Report

Declaration of Originality

Full names of student: Karabo Rathebe

Student number: 11214491

Declaration

1. I understand what plagiarism is and am aware of the University's policy in this regard.
2. I declare that this dissertation is my own original work. Where other people's work has been used (either from a printed source, Internet or any other source), this has been properly acknowledged and referenced in accordance with departmental requirements.
3. I have not used work previously produced by another student or any other person to hand in as my own.
4. I have not allowed, and will not allow, anyone to copy my work with the intention of passing it off as his or her own work.

Signature Of Student:.....

Signature Of Supervisor: *J Bester*

Chapter One

Introduction

Alzheimer's disease (AD) is a progressive, neurodegenerative disease that is characterised by the late-stage progression of the loss of cognitive abilities, particularly memory loss. It is fifth leading cause of deaths in the United States, but it is also the cause the leading cause of morbidity and disability in the older adult population¹. Alzheimer's disease is expected to increase in prevalence as the world population becomes older and life expectancy increases over time, resulting in AD becoming a significant clinical and financial burden².

It is now agreed that there are two core pathologies of AD: tau protein hyperphosphorylation and the formation of amyloid- β plaques. While these pathologies are considered the hallmarks of AD, the exact mechanism of their pathogenesis and the subsequent clinical manifestation of dementia and spatial memory loss are not well understood to this day. One of the only mechanisms that has been able to explain the prevalence of AD pathology is chronic systemic inflammation^{2,3}.

Due to the fact that inflammation, in particular neuroinflammation, has been shown to play an important in the pathogenesis of AD, it has been suggested that the neuroinflammation causing AD pathology could have originated elsewhere in the body². This suggestion is further supported due to the prevalence of secondary illnesses in those diagnosed with AD, such as cardiovascular and respiratory illnesses. It is thought that co-morbidities may be masking the actual number of people who are affected with AD¹. It may be that the systemic inflammation starts in another organ in the body, and the continued systemic inflammation enters the circulation and finally bypasses the blood-brain barrier. An emerging theory suggests that AD pathogenesis might be a combination of neurological and metabolic complications that are often seen in these patients, the gut-liver axis theory.

The liver is a versatile organ, carrying multiple functions, such as metabolism and clearance of toxins. However, its main function is the regulation and surveillance of immunity. Of particular interest is its role in the maintenance of immunological haemostasis, through the production of coagulation factors. Its positioning is also a factor, as it is situated at a point where the arterial and venous blood flow coincide. Portal circulation accounts for about 30% of the total blood flow, enabling the liver to screen for both systemic and gut-derived pathogens; therefore the liver is considered to be in a consistent but regulated state of inflammation^{13,14}.

Lipopolysaccharide, or LPS, is an endotoxin that has been shown to be a key modulator of the innate immune response, and has been extensively used as a means to conduct research into the pathology of neurodegenerative diseases, particularly AD¹⁰, with several animal models inducing inflammation by administering low concentrations of LPS into rats or mice over a specific period of time to in an attempt to mimic or reproduce the pathogenesis of AD^{7,8,10}.

It has been suggested that dysbiosis in liver haemostasis can result in translocation of pathogens into the systemic circulation, which may result in these pathogens being spread elsewhere in the body, particularly the brain. Changes in liver haemostasis may induce an inflammatory response and could result in an increase in the production of several inflammatory cytokines and ultimately affect the liver's function in coagulation production. In response to this dysbiosis, the liver would enter a state where certain coagulation factors increased due to a state of chronic inflammation. This may lead to liver injury and could result in liver fibrosis^{19,20,21}.

While there have been studies that have established the link between inflammation, LPS and AD disease progression, the idea that this inflammation may have originated elsewhere has not been the focus of research. Therefore, the current study aims to investigate the effects of systemic LPS on liver morphology and function, with particular focus on the production of coagulation factors. This will be achieved by the use of three techniques: light microscopy to examine the morphological changes of the liver tissue; TEM to examine the ultrastructural changes; and by determining the effects of LPS administration on the levels of tissue factor (TF) and fibrinogen by using ELISA assays. In addition, behavioural testing will be conducted to determine the prescience of neurological deficits (short-term memory loss and cognitive decline) in the animals that are prevalent in an AD population.

Chapter Two

Literature Review

Chapter Objectives

This chapter will outline the available literature and past research in line with the title of the study.

2.1 Alzheimer's disease: a brief overview

Alzheimer's disease is a neurodegenerative disease that is the most common form of dementia, accounting for an estimated 60 – 80% of all cases¹. and is characterized by progressive cognitive decline. This decline is known to be a result of two hallmark pathologies: the formation of amyloid β plaques and neurofibrillary tangles in the brain^{1,2}. The pathogenesis of AD is still not clearly defined, but neuroinflammation is now well established as an important hallmark of AD pathogenesis^{3,4}. Several studies have sought to elucidate the importance of inflammation in neuropathology, and one avenue of research has been the use of lipopolysaccharide (LPS), or endotoxaemia, to induce and mimic the pathogenesis seen in AD. Inflammation induces the release of pro-inflammatory cytokines by immune mediators in the brain, such as microglia and astrocytes, which causes the cognitive and memory deficits seen in AD patients⁵. There is also increasing evidence of links between AD and vascular risk factors, such as hypoperfusion and atherosclerosis, giving rise to the suggestion that the pathogenesis of AD may also be due to vascular mechanisms⁶.

2.2 Lipopolysaccharide and Alzheimer's disease

Lipopolysaccharide (LPS), also referred to as endotoxin, is the main component in the outer membrane of Gram-negative bacteria, such as is seen in *E.coli*. It contains three components, a polysaccharide that contains an O-antigen, an outer core and an inner core, which is anchored to the outer membrane by a lipid, known as Lipid A, the element of LPS that can induce toxicity in the host cell (Figure 2.1). Lipopolysaccharide acts as a strong stimulator of the innate immune response, due to the presence of pathogen-associated molecular patterns (PAMPs) found on lipid A, which binds to Toll-like receptors found on host cells⁶. This stimulates the release of various pro-inflammatory cytokines and chemokines, such as Tumor necrosis factor (TNF)- α and Interleukin (IL) 1- β , and oxygen free radicals, such as nitric oxide (NO), contributing to induce systemic inflammation⁷⁻⁹.

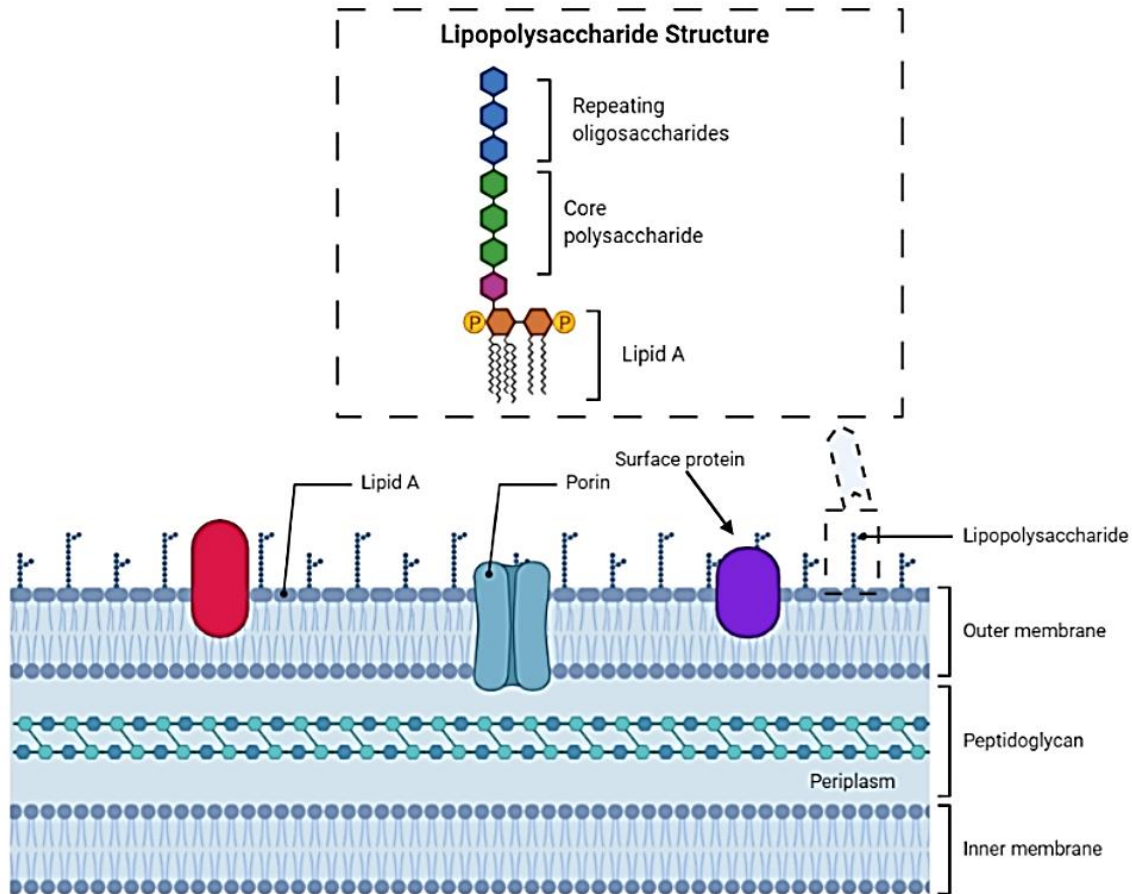


Figure 2.1 The structure of a Gram negative bacterial cell wall (a), showing the location of lipopolysaccharide, and its structure (b). Created with BioRender.com.

Systemic inflammation has been shown to be a major factor in the progression of several non-communicable diseases, like AD, due to the damage caused to vital organs as a result of the various physiological changes brought about by consistent, low-grade stimulation of inflammatory pathways. The liver is likely to be the first organ to be exposed to effects of LPS. The link between how LPS reaches the liver, and its metabolism was presented by Nolan as the leaky gut theory¹⁰⁻¹¹. This theory states that the presence of LPS results in the breakdown of the barrier that prevents bacterial translocation into the circulation, allowing for LPS to be absorbed into the portal circulation through the intestine, and into the liver via the portal vein, thus stimulating an immune response in the liver¹⁰. Hence, the liver serves as an important buffer between the gut and the systemic circulation, characterised as gut-liver axis. Dysbiosis (microbial imbalance) in the gastrointestinal tract can lead to bacterial translocation from the intestinal tract into the circulation,

due to the dysfunction in the endothelial barrier. Once this occurs, bacteria can bind to their respective pathogen receptors, triggering an immune response¹².

2.3 Inflammation and liver function

The liver plays an important role in serving as a buffer between the systemic circulation and gut-derived contents, with 80% of hepatic blood supply being delivered to the liver from the gut via the portal vein. It is now considered as the 'immunological organ', owing to function in immunity. The liver is responsible for the production of modifiers and inducers of innate immunity, including the acute phase protein, chemokines and cytokines, from a variety of resident immune cells. Due to the fact that it is exposed to a stream of bacterial products, as well as the stimulation from continual changes in metabolic activity, the liver is in a persistent, yet regulated state of inflammation¹³. The immune cells that induce and modulate the immune response in the liver include Kupffer cells (KCs), hepatocytes and liver sinusoidal endothelial cells (LSECs). Each has its own function, from scavenging and filtration (LSECs and KCs), liver regeneration and tissue repair (KCs), and the clearance of toxins and bacteria in the circulation (hepatocytes). These cells are the main producers of pro- and anti-inflammatory cytokines, namely IL-6, IL-10, IL-1 β and TNF- α ¹⁴⁻¹⁶.

Circulating LPS has been shown to affect changes in the acute phase response (APR), particularly at lower levels than would be expected, as a result of the nature of portal blood circulation. Knolle and colleagues showed that by introducing low concentrations of LPS (100pg/ml to 1ng/ml) in hepatocytes induces the release of IL-6, which initiates APR in the liver¹⁷. IL-6 is an especially important cytokine, as it is the initial mediator of APR, and its continuous production can lead to the development of systemic, chronic inflammation.

Immunological function of the liver strives to maintain systemic homeostasis, through a tightly controlled process, any failure to clear toxic stimuli and pathogens can lead to deregulated homeostasis and chronic inflammation. One aspect of the liver's inflammatory functions is the development, and subsequent resolution of fibrosis. Resolving fibrosis is essential for liver wound repair in the event of injury, as well as the restoration of tissue homeostasis. The release of inflammatory cytokines (IL-6, TNF- α) during APR leads to the recruitment and activation of leukocytes that influence the induction of fibrotic responses at the site of inflammation. This, in

turn, leads to the activation of hepatocyte stellate cells (HSCs). HSCs are potent producers of the extra cellular matrix components that are seen in fibrosis, such as type 1 collagen and α -smooth muscle actin¹⁸⁻¹⁹.

Liver fibrosis is usually considered to be a feature of liver pathology, but is an important feature of liver homeostasis, and only becomes clinically relevant when it alters structure and function due to systemic inflammation. Persistent activation of inflammatory molecules maintains HSC-derived fibrosis, and a lack of resolution can lead to progressive liver fibrosis, resulting in the breakdown in the balance between inflammation and tissue homeostasis (Figure 2)^{13,19}.

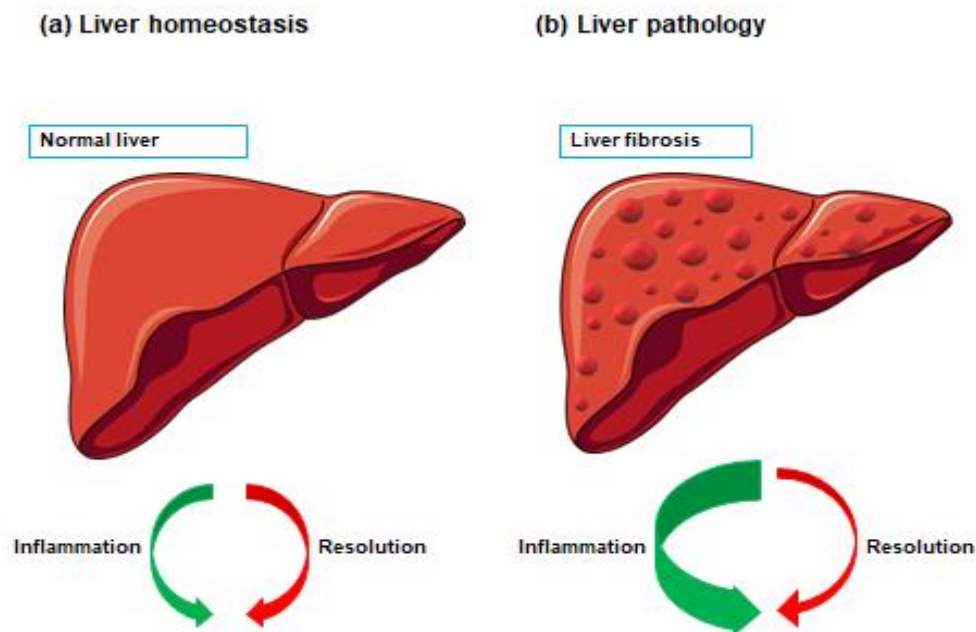


Figure 2.2 The balance between inflammation and tissue homeostasis in the liver. Changes or failure by the liver to effectively clear toxic substances, coupled with the resolution of fibrosis, leads to impaired liver function and tissue damage¹¹. Liver homeostasis ensures that the liver regenerates, maintains tolerance to LPS and that there is resolution of fibrosis (a). Injury or infection results in homeostasis being lost, and the occurrence of increased inflammation, and reduced ability to resolve fibrosis. This pathological state will result in liver damage and, ultimately, cirrhosis (b). Adapted and redrawn from reference 13

2.3.1 Inflammation and coagulation

The liver is also involved in the cascades that control blood coagulation, with all coagulation factors being produced by the liver, excepting von Willebrand factor. The classical model of coagulation was previously described as a cascade of reactions that occurred along an extrinsic and intrinsic pathway, which resulted in the production of thrombin and the subsequent fibrin formation. However, the cascade model did not adequately describe the mechanisms of haemostasis *in vivo*, nor does it explain the pathophysiology of haemostasis in some conditions, such as Haemophilia²⁰. To remedy the gaps in knowledge caused by the traditional cascade model, Hoffman and Monroe²¹ developed the cell-based model of haemostasis. This model proposed that cells played a more important role in coagulation than previously thought, meaning that coagulation would be controlled by cellular components and the properties of cell surfaces, rather than the interactions between coagulation proteins.

Instead of occurring along distinct pathways, the cell-based model of haemostasis is overlapping steps, consisting of initiation, amplification and propagation. Tissue factor is known to be the main initiator of coagulation according to this model, as most cells that express TF are found outside the vasculature²²⁻²³. The process of haemostasis usually involves a latter step of the conversion of fibrinogen into fibrin, mediated by thrombin. Fibrin then polymerizes to form a clot. The ensuing anti-coagulation pathways that induce fibrinolysis are initiated by plasmin, degrading the fibrin molecules in order to destabilise the clot²⁴⁻²⁵. Fibrinolysis is an important mechanism that prevents excessive clot formation (Figure 2.3)²⁶. Disruptions in the balance between inflammation and coagulation can lead to catastrophic events, which will be discussed in later sections of this review.

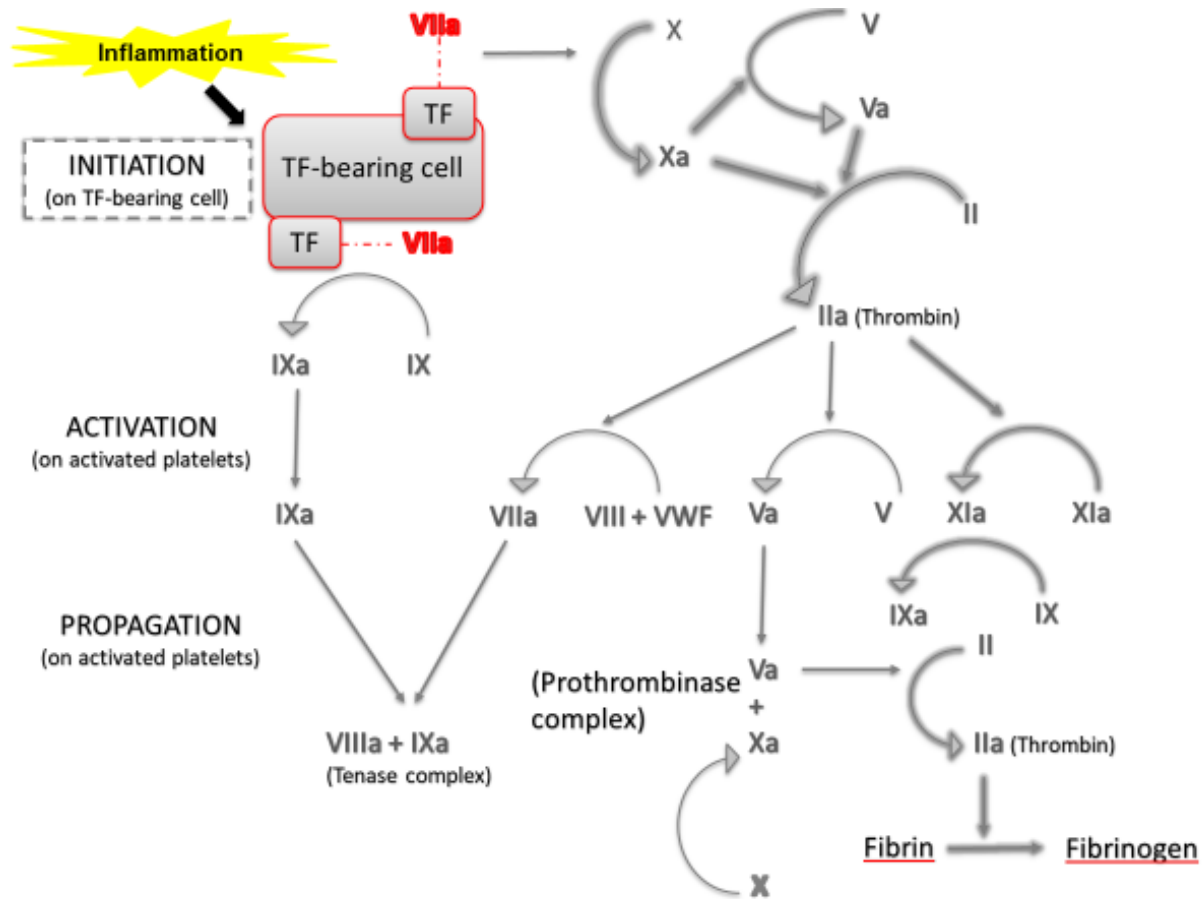


Figure 2.3 The cell-based model of haemostasis (including fibrin formation), differentiated into three overlapping phases: initiation, amplification and propagation. It begins with initiation phase, where tissue factor binds to factor VIIa to form the TF-VIIa complex. Amplification occurs when there is damage to the vasculature, subsequently activating the coagulation factors, and ultimately resulting fibrin clot formation. For this study, emphasis will be placed on the initiation and amplification phases after tissue injury, and the effects of inflammation on the liver's functioning in coagulation, as indicated by the grey-highlighted font. The coagulation factors that will be focused on are indicated with red underlining/outline.

The liver produces the many coagulation factors, such as factors II (or thrombin), V, VII, VIII, X, XI, XII, XIII and fibrinogen. It also produces the anti-coagulant factors, such as antithrombin, proteins C and S. Alterations in the production of CFs leads to a propensity for bleeding and simultaneous thrombosis in the event of liver dysfunction. Impairment of liver function can result in the decrease in CF production, excepting factor VIII (FVIII), which has been shown to be increased in cases of liver dysfunction and disease. Elevated FVIII leads to thrombin generation, which has been associated with increased venous thromboembolism. Fibrinogen initially

increases in liver disease, but will later decrease as liver disease progresses due to reduced hepatocyte production^{24,27}.

One important effect of liver dysfunction or disease is the decreased fibrinolysis, which occurs as a result of the decrease in the levels of the anti-coagulant factors, proteins C and S, and antithrombin. Patients with liver disease present clinically with increased bleeding as result of the disruptions of the functions of the liver in coagulation²⁷. There is evidence that inflammation and coagulation are involved in cross-talk between each other; inflammation influences coagulation, and in turn, coagulation influences inflammation in a positive feedback manner. However, chronic inflammation can lead to impaired coagulation contributing to disease²⁸. The failure of anticoagulants in stopping the process of coagulation and clot formation can result in persistent coagulation and vascular thrombosis²⁹⁻³⁰.

2.3.1.1 Cross-link between coagulation and inflammation: Role of tissue factor and fibrinogen

Tissue factor is a major initiator of the initiation phase of coagulation, binding to factor VII to form a complex that initiates clot formation, acting as a pivotal initiator for inflammation-induced thrombin generation. Tissue factor is also considered to be a driver of inflammation, with studies showing that circulating mononuclear cells express TF, resulting in system activation of coagulation in severe sepsis^{29,31}. Franco and colleagues also provided evidence of this in a low-dose endotoxaemia model, with the levels of TF mRNA levels increasing after low doses of LPS were injected in patients. This shows that not only is TF expression a crucial element of coagulation after vascular injury, it also plays a part in maintaining haemostasis and the inflammatory response³².

The main feature of the initiation pathway is the formation of the TF/FVIIa complex, which in turn leads to thrombin generation, and ultimately, the conversion of fibrinogen into fibrin. Fibrin clot formation, and the subsequent fibrinolysis mediated by anti-coagulant factor, is an essential component of maintaining haemostasis. It has been suggested that coagulation modifies the progression of liver disease, particularly through fibrogenesis via the continued expression of fibrinogen^{31,33-34}. There are, however, different theories on how the coagulation cascade influences the progression of hepatic fibrogenesis. Anstee and colleagues³⁵ reviewed the two hypotheses that are most likely to explain hepatic fibrogenesis, namely parenchymal extinction

caused by tissue ischaemia, and direct thrombin-related hepatic stellate cell activation (Figure 2.4). While both hypotheses are able to explain the role of the coagulation cascade in the control of tissue repair and remodeling after injury, HSC activation has been proven by a number of studies that examined the mechanisms of fibrogenesis control in different organ systems apart from the liver, such as the lungs³⁵. Parenchymal extinction may be able to provide a link between the vascular events that lead to the loss of hepatocytes, and the subsequent development of fibrosis through HSC activation.

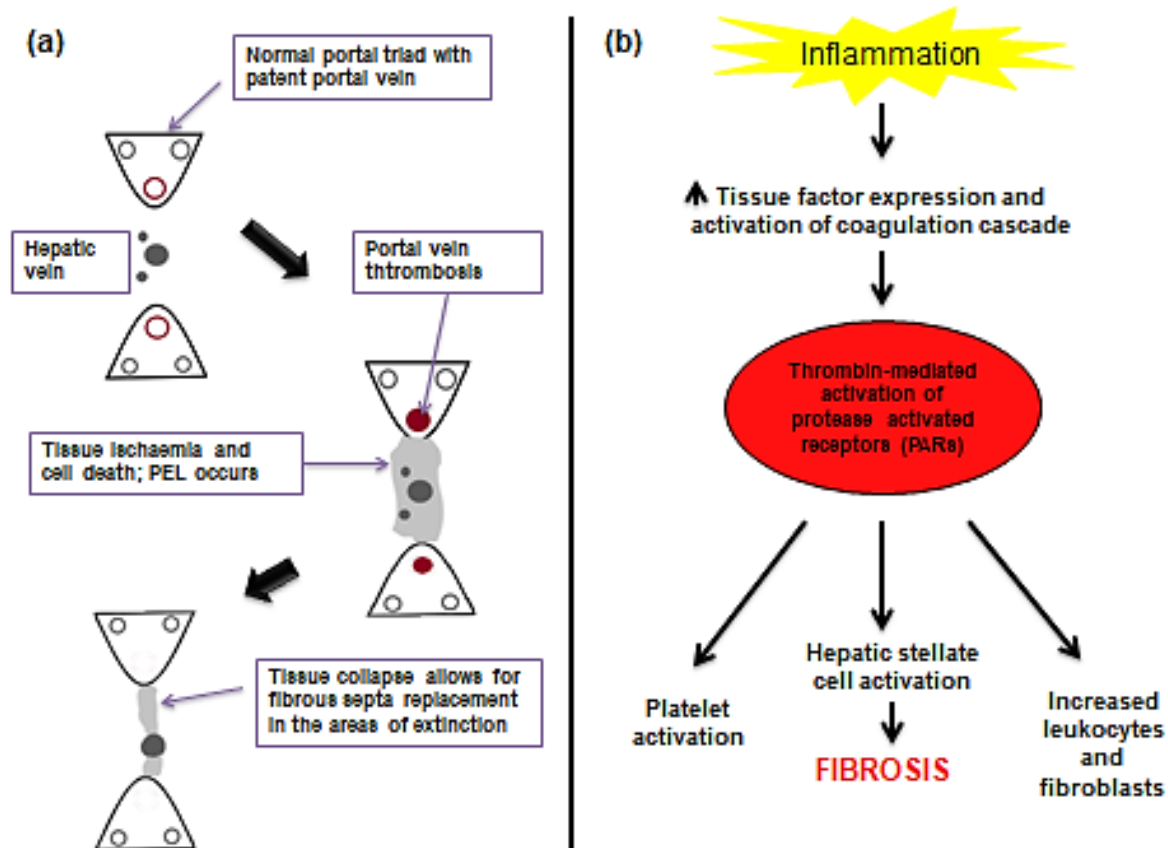


Figure 2.4 A schematic representation of the two hypotheses that are likely to explain the progression of hepatic fibrogenesis. (a) Parenchymal extinction due to portal vein thrombosis. This thrombotic event leads to tissue ischaemia and cell death. The tissue surrounding the hepatic vein collapses, allowing for fibrous septa to replace what tissue was apparent before extinction. (b) Direct activation of hepatic stellate cells via thrombin-mediated PAR signaling, leading to fibrosis. This also leads to other, related complications of systemic inflammation, including increased platelet activation and increased release of leukocytes and fibroblasts. Adapted and redrawn from reference 35.

An increase in the levels of fibrinogen is considered an indicator of a pro-inflammatory state. It has been identified as a marker for the development of pathological thrombotic events³⁵. Lipopolysaccharide administration has been shown to have an effect on thrombin, triggering intravascular thrombosis via tissue factor expression, resulting in fibrogenesis and deposition in the hepatic sinusoids³⁶. Due to the fact that the initiation pathway is dependent on the occurrence of tissue injury, it should follow that the region in which injury occurred should be the location of fibrinogen deposition. In an investigation of the role of TF in a mouse model of endotoxaemia, Pawlinski et al³⁷ showed that the TF expression is driven mainly by monocytes that are found in the endothelium³⁷. Liver sinusoids contain several cell types, including hepatocytes and HSCs. It can therefore be suggested that any change in TF expression by these cells, particularly in an LPS-induced inflammatory state, can contribute to fibrogenesis, the subsequent malfunction in coagulation and the development of liver disease and cirrhosis³⁶.

2.4 Hypercoagulability: pathogenesis and consequences

One of the hallmarks of chronic or systemic inflammation is hypercoagulability (HC), the abnormally increased tendency to blood coagulation (blood clotting)³⁸. Hypercoagulability is characterized by pathological haemostasis, namely increased production of coagulation factors, decreased fibrinolysis, hyper activated platelet and vascular defects³⁹. As liver disease progresses, the development of a hypercoagulable state results in the decrease in circulating levels of coagulation factors and anti-coagulant proteins, the occurrence of thrombocytopenia and altered platelet function (abnormal platelet adhesion to the site of injury)^{35,40}. The complications seen in liver disease are characterised as a paradox, as haemostasis has lost the balance between coagulation and bleeding, but results in both an increased tendency to bleed as well as abnormal clotting⁴⁰.

2.4.1 The hypercoagulable state in Alzheimer's disease

Neuroinflammation is a known and proven part of the pathogenesis of AD. However, AD is also considered to be a systemic inflammatory condition, as affected individuals present with abnormal changes to their innate immunity and inflammation processes, resulting in abnormal changes in organ function.

As the liver is the main organ that produces coagulation factors (apart from vWF), it is also an important player in inflammation; therefore, it can be said that inflammation and hypercoagulability are interlinked³⁹. The main characters that seem to be involved are IL-1 β and IL-6, particularly the mechanism that involves the activation of IL-6 and the resulting induction of fibrinogen synthesis by hepatocytes^{25,41}. In AD patients, HC is closely associated with an increase in fibrinogen, which has been shown to be implicated in the development of neuroinflammation and memory deficits⁶.

Lipopolysaccharide has been suggested to play a role in the occurrence of HC in AD patients, and its structure may explain the development of the hypercoagulable state, as well as hypofibrinolysis in inflammatory diseases⁴². Pretorius and colleagues⁴³ found that adding small concentrations of LPS to whole blood and platelet-poor plasma caused changes to the formation of fibrin fibres, which resembled changes seen in inflammatory diseases that had LPS involvement as a cause of the disease. The same study also found that the critical stage of the common pathway, the polymerisation of fibrinogen into fibrin fibres, is affected by LPS exposure. The study hypothesised that LPS binds directly to fibrinogen, changing the structure of the fibrin clot, thereby causing abnormal clotting⁴³.

2.4.2 Linking hypercoagulability and liver dysfunction

One of the effects of the hypercoagulable state seen in AD is hypofibrinolysis, the subsequent binding of LPS and fibrin and abnormal clotting. An increase in fibrin in the liver may lead to liver fibrosis, causing damage and further affecting liver function⁴⁴. Hypercoagulation also causes an increase in the formation of amyloid, an important feature of AD pathogenesis, as seen in the formation amyloid β plaques in the brain^{3,44}. Amyloidosis is a common pathological feature in liver disease, further demonstrating another possible link to hypercoagulability in AD and organ failure⁴⁵⁻⁴⁷.

It is possible to deduce that because the liver plays such an important role in coagulation and inflammation, any abnormality that may occur can also affect the liver, causing damage. Therefore, LPS-induced inflammation causes the increased production of pro-inflammatory cytokines, which further impair the coagulation cascades. Impairment of coagulation leads to microvascular thrombosis, hypoperfusion (or inadequate oxygen uptake), ultimately resulting in organ failure. Lipopolysaccharide plays an important role in the development of systemic

inflammation in AD, and hypercoagulability is a hallmark of inflammation; therefore, it can be deduced that the hypercoagulability in AD is involved in causing liver damage, and subsequent liver failure.

The aim of this study was to investigate the effect of systemic LPS-induced inflammation within aged Sprague-Dawley rats on liver morphology and function, specifically focusing on the production of TF (Factor III) and fibrinogen (Factor I) and the possible contribution to HC in AD. Various microscopic techniques (these methods are outlined in Chapter 3) were used to study the morphological changes in the liver and correlated back to the effect on liver function. Also, the concentration of TF and fibrinogen were measured to determine whether this contributes to the hypercoagulable state of AD patients.

The following objectives will direct this thesis:

1. To study the ultrastructural morphology to determine liver damage between the treated and control rat groups using transmission electron microscopy.
2. To study the morphology of liver tissue damage using light microscopy by Haematoxylin and eosin, Picrosirius red and Congo red staining.
3. To determine the concentration of coagulation factors (TF and fibrinogen) using ELISA assays.

Chapter Three

Establishment of the Sprague-Dawley rat model of systemic and neuroinflammation in Alzheimer's disease

3.1 Chapter Objectives

The objectives of this chapter are to implement a rat model of systemic and neuroinflammation in AD that results in a Sprague-Dawley rat population displaying Alzheimer’s-like features, particularly chronic inflammation.

3.1.1 Ethical considerations

Ethical approval for this study was obtained from the Faculty of Health Sciences Research Ethics Committee at the University of Pretoria, reference number 176/2020. Further approval was obtained from the Animal Research Ethics Committee at the University of the Witwatersrand, clearance certificate number 2019/07/44/C. To ensure the welfare of the rats during the course of the experimental period, particularly due to the fact that the objectives of the study required the animals undergoing a significant amount of stress. An outline of the methods and techniques used in this study is shown in figure 3.1

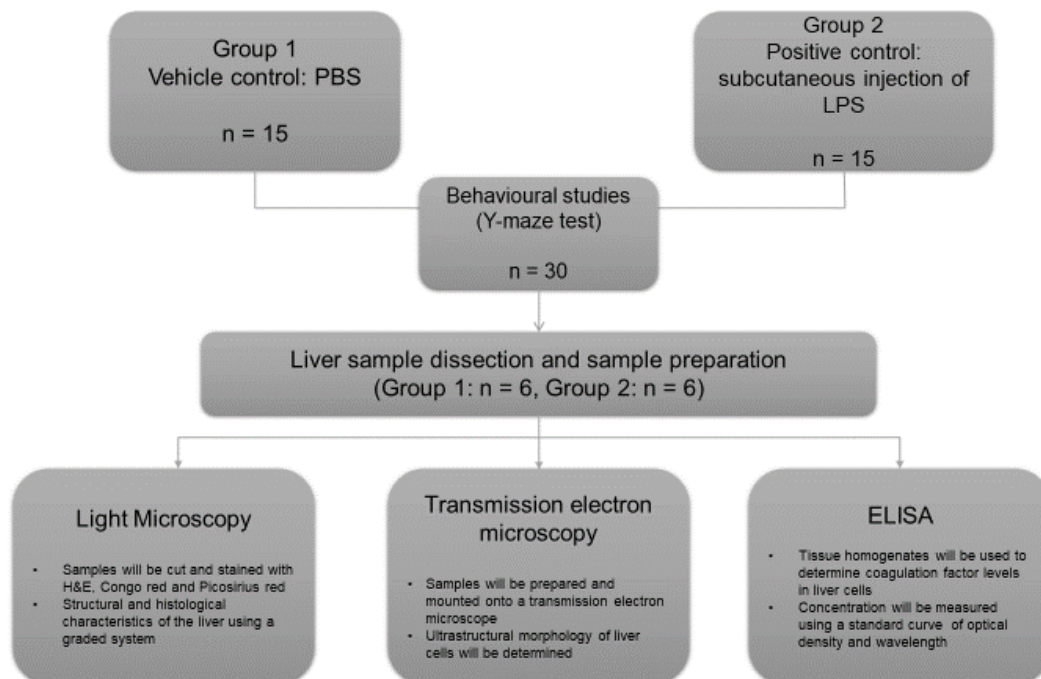


Figure 3.1 An overview of the experimental design of the study, as well as the methods used to achieve the objectives of the study.

3.2 Methods and Materials

3.2.1 Materials

This study used 8 weeks old male Sprague-Dawley rats that were exposed to daily injected doses of solutions of PBS and LPS.

- LPS (E coli 055:B5, Sigma-Aldrich)
- Phosphate buffered saline (PBS) (Sigma-Aldrich)
- 12 male Sprague-Dawley rats (Central Animal Services, Wits)
- 5 mL glass vials (Lasec)
- 10 mL Syringes and needles (provided by central Animal Services, Wits)
- Plexiglass Y maze (provided by Central Animal Services, Wits)

3.2.2 Methods

3.2.2.1 *Implementation of the model*

Eight-week-old Sprague-Dawley rats, with an average weight of 250-300 g, were maintained at the Central Animal Services (CAS) unit at the University of the Witwatersrand. The rats were conventionally housed in alternating cages of pairs and triplets per cage and sawdust was used as bedding material, with cage sizes as per the SANS 10386:2008 recommendations (Figure 3.2). The rats were provided with standard irradiated “Epol” rat pellets and municipal water ad libitum. Room temperature was maintained at 25 - 27°C, with a relative humidity of 50% (\pm 20%) and a 12-hour night/dark cycle throughout the course of the study. The rats were randomly divided into two experimental groups, with each group containing six rats. They were allowed to acclimatise to their environment for 7 days prior to dosage, after which the experimental period began, continuing for a further 10 days. The final stage of the housing period involved the behavioural testing to establish that the rats were representative discomfort of an Alzheimer’s-like population over a period of 2 days. Therefore, the total housing period of the rats was 19 days. The dosages for the PBS and LPS are indicated in Table 1 and were administered via subcutaneous injections daily for a period of 10 days. The animals were handled and injected by the veterinarian nurses and technicians at the CAS unit.



Figure 3.2 Layout of the rat's housing during the acclimatisation and experimental periods. The control and experimental groups are shown on the top row of the figure.

The measurement of the weight of the rats was not a primary objective of this study. However, this measurement was used to track the welfare of the rats during the experimental period, along with other methods that were mandated by the CAS unit.

The welfare of the rats was measured against several characteristics outlined in the Rat Grimace Scale (Figure 3.3), along with the daily measurement of weight on the first day of the acclimatisation period thereafter, weight was measured daily during the experimental period. At any point during the experimental period if a rat's weight decreased at a rate of more than 15% of its weight at the start of the acclimatisation period, it would have to be removed from the study.

NC 3R^s National Centre for the Replacement, Refinement & Reduction of Animals in Research

The Rat Grimace Scale

Research has demonstrated that changes in facial expression provide a means of assessing pain in rats.

The specific facial action units shown below have been used to generate the Rat Grimace Scale. These action units increase in intensity in response to post-procedural pain and can be used as part of a clinical assessment.

The action units should only be used in awake animals. Each animal should be observed for a short period of time to avoid scoring brief changes in facial expression that are unrelated to the animal's welfare.

	Not present "0"	Moderately present "1"	Obviously present "2"
Orbital tightening <ul style="list-style-type: none"> Closing of the eyelid (narrowing of orbital area) A wrinkle may be visible around the eye 			
Nose/beak flattening <ul style="list-style-type: none"> Flattening and elongation of the bridge of the nose Flattening of the cheeks (potentially sunken look) 			
Ear changes <ul style="list-style-type: none"> Ears curl inward and are angled forward to form a 'bushy' shape Space between the ears increases 			
Whisker change <ul style="list-style-type: none"> Whiskers stiffen and angle along the face Whiskers may 'clump' together Whiskers lose their natural 'downward' curve 			

Read the original paper: [Bancroft JR, Sorge RE, Dobson A, Tuttle AJ, Marini LJ, Weening JF, Mapplebeck JC, Wei R, Zhou B, Zhang B, McDougall JJ, King GD, Mogil JS. 2011. The Rat Grimace Scale: a partially automated method for quantifying pain in the laboratory rat via facial expressions. *Molecular Pain* 7:55. doi:10.1186/1745-0213-7-55](#)

For guidance on using the Rat Grimace Scale, research papers that describe this technique and for grimace scales in other species, visit www.nc3rs.org.uk/grimacescales. To request copies of this poster, please email nc3r@nc3rs.org.uk. The NC3Rs provides a range of 3Rs resources at www.nc3rs.org.uk/resources.

Images kindly provided by Dr Jeffrey Mogil, McGill University

Figure 3.3 The Rat Grimace Scale used to check the welfare of the rats throughout the experimental period⁴⁸.

Lipopolysaccharide was administered at low physiological doses to mimic the systemic release of LPS in the body while maintaining systemic inflammation and limiting the amount of experienced. The LPS was given to stimulate chronic systemic inflammation, similar to the neuroinflammation experienced in AD. The vehicle control group was administered daily

subcutaneous injections of 0.1 M PBS at a volume of 0.1 mL per kg of rat for 10 days. Experimental group will be administered a daily SC injection of LPS (*E. coli* 055:B5; Sigma-Aldrich) dissolved in PBS at a concentration of 0.1 mg/mL at a volume of 0.1 mL per kg of rat.

Table 3.1 Control and experimental group dosages

<u>Group</u>	<u>Intervention</u>	<u>Dosage</u>
PBS (vehicle control)	0.1M PBS	0.1 mL/kg/rat
LPS	<i>E. coli</i> 055:B5	[0.1 mg/mL]
		0.1 mL/kg/rat

3.2.2.2 Observations made during the experimental period

The animals were monitored on a daily basis by the student investigators involved in the project, with further monitoring by a registered veterinary technician and the chief veterinarian of the CAS unit. Each dose of LPS and PBS was calculated according to the weight of each animal that was obtained on a daily basis, in order to inject the correct dose into each animal. The average weights of the rats ranged between 300 - 500 g.

3.2.2.3 Behavioural studies

Before termination, the rats underwent behavioural analysis using the Y maze test. The Y maze test was chosen as it is a good indicator of spatial and short-term memory, as well as anxiety in rats⁴⁹. Prior to testing, the animals were moved to the testing room in order for them to acclimatise to the environs of the room. The Y maze consist of three arms, one long and two shorter radial arms (Figure 3.4).

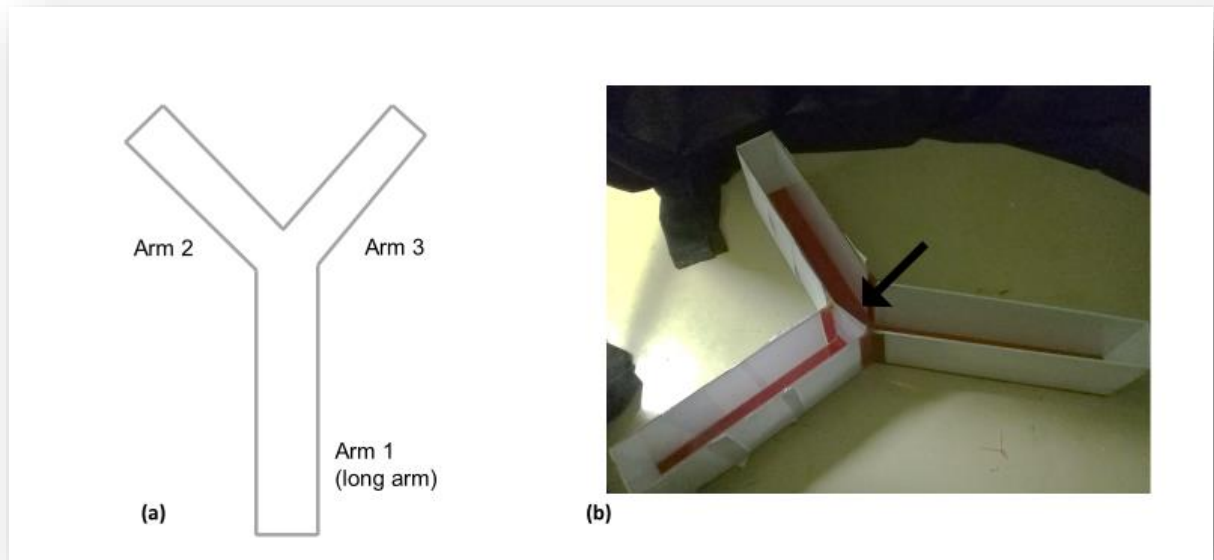


Figure 3.4. a) A schematic drawing representing the Y maze apparatus used during behavioural testing. b) A photograph of the actual experimental room and setup during the habituation phase. The barrier in front of one of the arms of the apparatus is visible (indicated with an arrow).

The animals were tested in morning during their light cycle to ensure that were alert during testing. The testing was carried out in two phases: a habituation phase of 3 minutes and a testing phase of 3 minutes, totalling 6 minutes. The habituation phase consisted of placing a rat in one arm (in this case the long arm), with one radial blocked for entry. Each rat was allowed to explore the two remaining arms for 3 minutes. For the testing phase, the block was removed, and each rat (one at a time) was placed into the Y maze and allowed to freely explore all three arms for 3 minutes (Figure 3.5). The amount of time spent in the unblocked arm was recorded. After each trial, the Y maze was cleaned, disinfected, and dried before placing the next animal.

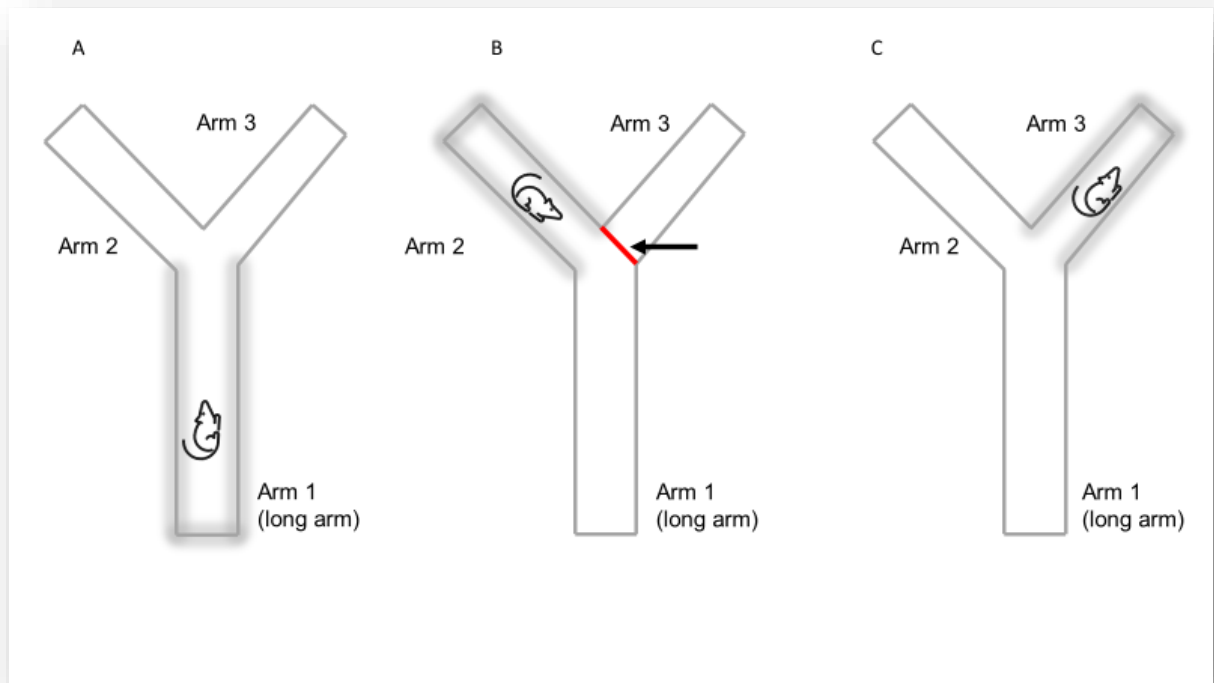


Figure 3.5. A representation depicting the different entries into each arm of the y maze. Each entry is highlighted in grey. The animals were first placed, one at a time, into the long arm of the Y maze apparatus, then allowed to explore the apparatus. A barrier (shown in red and indicated with an arrow) was placed in front of the entrance to arm 3 during habituation, in order for each animal to become acclimatised to the environment. For the testing phase, this barrier was removed, and each animal's willingness to enter arm 3 was then tested, according to the time spent in each arm. Drawn and adapted from Prieur and Jadavji⁵⁰.

3.2.2.4 Termination

The rats were terminated by decapitation. Each animal was first be exposed to Halothane for 30 seconds, as an anaesthesia, followed by perfusion with saline and a 4% formalin solution and decapitation. All of the above steps were conducted by a registered veterinary technician. This method of termination was used to limit the amount of changes imposed on the tissue of interest as well as to the coagulation system.

3.2.2.5 Tissue sample collection

After termination, the liver was removed and cross-sections of the right medial lobe, the left lobe and the caudate lobe were dissected. These sections were then fixed in a 4% formaldehyde

solution diluted in PBS, and further prepared for light and TEM analysis. The sections were also homogenized in T-PER protein extraction buffer (Thermo Fisher Scientific, South Africa) containing complete protease inhibitor (Sigma-Aldrich, South Africa) and phosphatase inhibitor (5 mM sodium fluoride and 50 μ M sodium orthovanadate) and centrifuged at 16,000 θ for 20 minutes at 4°C. The supernatant containing the soluble protein fraction was collected as the detergent-soluble fraction, stored at -80°C and used for ELISA assays. The methods for each technique are described below.

3.2.2.5.1 Light microscopy

The harvested liver tissue was cut into samples of approximately 5 mm³ size, then fixed in 4% formaldehyde overnight. The samples were then rinsed three times with 0.1 M PBS for 15 minutes each time, then dehydrated with ascending concentrations of ethanol (Sigma-Aldrich), 50%, 70%, 90% and 100% twice. The tissue was then left in 100% ethanol overnight. The samples were then placed in *tert-butyl* alcohol (TBA; Sigma-Aldrich) for two days, renewing the TBA three times a day. After this, wax pellets were added to the TBA to create a 50:50 TBA-wax mixture, which was then added to the samples. The samples in the TBA-wax mixture were then left in an oven for 2 days at 60°C, renewing the TBA-wax mixture three times a day. The samples were then transferred to a 100% wax solution for 24 hours at 60°C. Finally, the samples were placed in a steel mould, filled with wax and a plastic, marked grid/cassette placed on top. The samples with the grids were cooled to 4°C by placing them on a cooling plate to allow them to harden. Sections of between 3 - 5 μ m thickness were cut with a microtome and placed on slides. *Tert-butyl* alcohol wax embedding was done instead of the normal embedding containing xylene, due to previous evidence of the normal paraffin embedding process resulting in impaired tissue infiltration and irregular sectioning of liver samples⁵¹.

3.2.2.5.2 Transmission electron microscopy

Tissue samples were cut into 1 mm³ cubes and added to vials containing 2.5% glutaraldehyde/formaldehyde solution to fix for a period of 1 - 24 hours. Once fixed, the fixative was removed, and the samples were washed with PBS (Sigma-Aldrich) 3 times, each for 15 minutes. In a fume cupboard, a secondary fixative, 1% Osmium Tetroxide (Advanced laboratory solutions) solution was added to the samples for 1 hour. Thereafter, the fixative was removed by washing the samples with PBS three times, each for 15 minutes (the first wash with PBS was

done in a fume cupboard, to ensure safety). The samples were then dehydrated with ascending concentrations of ethanol (30%, 50%, 70%, 90% and three changes of 100%) for 15 minutes each concentration, the last dehydration with 100% ethanol being left for 30 minutes. The ethanol was then removed, and the samples were added to propylene oxide (PO), three times for 15 minutes. The samples were then added to a 2:1 mixture of PO and resin for 1 hour, thereafter they were added to another 1:2 solution of PO: resin for between 2 - 4 hours. This solution was then removed, and the samples were then embedded in 100% resin. Once the embedded samples were hardened in a 60°C oven for 36 hours, they were cut into ultrathin sections using an ultramicrotome. The samples were then stained with uranyl acetate and lead citrate for contrast, and then examined using a JEOL JEM 2100F transmission electron microscope (JEOL USA, Inc)

3.2.2.5.3 ELISA

Detection of the levels of TF and fibrinogen in homogenized liver tissue samples were done using the Rat TF ELISA kit (The Rat tissue factor (TF)/ coagulation factor VII (F7) complex ELISA kit (My BioSource, MBS910833) and the Rat Fibrinogen ELISA kit (The Rat FG (Fibrinogen) ELISA kit (Elabscience, E-EL-R1125). For both assays, each protocol in the manual was followed. Each assay was done based on the sandwich-ELISA principle, where the micro-plate wells are pre-coated with a primary antibody specific to TF and fibrinogen.

The concentrations of TF and Fibrinogen was obtained by measuring the optical density of each sample, due to the colour-change reaction elicited by the assay. The optical density was measured with a microplate reader at a wavelength of 450 nm. A standard, logistic curve was used to extrapolate and measure the unknown TF and Fibrinogen concentrations.

3.2.2.6 Statistical Analysis

For analysis of the weights of the animals, raw data was collated in Excel, then transferred for analysis using the software GraphPad Prism 8. The mean and standard deviation of the weights was represented over the experimental period.

Chapter Four

Establishment of the Sprague-Dawley rat model of systemic and neuroinflammation in Alzheimer's disease: Behavioural Studies

4.1 Chapter Objectives

The objectives of this chapter are to implement a rat model of systemic and neuroinflammation in AD that results in a Sprague-Dawley rat population displaying Alzheimer's-like features, particularly the development of memory and cognitive impairment determined by neurophysiological behavioural studies.

4.1.1 Introduction

Research into the aetiology and pathogenesis of AD has undergone several changes and overhauls in recent years, particularly as there is still no clear agreement on how the disease develops, despite decades of intensive research into several models of neurodegeneration⁵². Animal models of the disease have become a critical tool in the research into AD, as these models can allow for the discovery of disease pathways and the development of new therapies and treatments⁴⁹.

Of particular interest is the use of behavioural animal models that mimic or simulate the decline in memory and cognition that are hallmarks of AD. Behavioural animal models can be characterised as spontaneous, induced negative and orphan models⁵². For this study, behavioural testing was used to confirm the prevalence of an Alzheimer's-like rat population as a result of the LPS-induced systemic inflammation (as discussed in chapters 2 and 3).

There are several behavioural tests that can be used and adapted to assess the memory and cognition of animals that are mostly based on the hippocampus' contribution to cognitive function, particularly spatial memory⁵⁴. The Morris water maze, the radial arm maze and the Y maze have all been shown to demonstrate the effects that hippocampal damage (whether through direct injury or any physiological change) can have on the spatial memory of rats.

The Y maze test was designed and described by Prieur et al, as a means of determining short-term spatial memory in adult and aged mice⁵⁰. The main premise of the Y maze test is a rat's innate tendency to explore a novel environment, otherwise known as spontaneous alteration. Spontaneous alteration is tied to an animal's willingness to explore its environment and locate resources such as food and water and is considered an appropriate indicator of hippocampal

dysfunction⁵⁵⁻⁵⁷. The Morris water maze has long been used as test for short-term spatial memory but is considered to cause more stress that may influence the interpretation of the results⁵⁴. The Y maze may be more ethologically relevant in determining the spatial memory of rats, due to the fact that there is less manipulation to the rats and the animals are more likely to explore the maze similarly to how they would explore their natural environment.

4.2 Methods and Materials

4.2.1 Materials

- 12 male Sprague-Dawley rats (provided by Central Animal Services, Wits)
- Plexiglass Y maze (provided by Central Animal Services, Wits)
- ANY-Maze software (provided by Central Animal Services, Wits)
- GraphPad Prism (statistical software)

4.2.2 Methods

The behavioural study testing procedure is described in chapter 3.

4.2.3 Statistical analysis

For the behavioural testing, the software ANY-Maze was used to carry out and measure the times spent in each arm of the Y maze apparatus, according to the demarcations set for each arm (Figure 4.1). The main outputs used for analysis were the number of entries each rat made into each arm, as well as the number of alterations, or the number of times the animals entered into all three distinct arms. A formula was then used to determine the ratio of alternations to the number of arms entered⁵⁰, which is represented as follows:

$$\% \text{ alterations} = \frac{\text{total number of alterations}}{\text{number of arms entered} - 2} \times 100\%$$

Unpaired t-tests were performed on the data to compare the experimental and control groups. In all the analysis, $P < 0.05$ was considered statistically significant, and the data was represented as mean \pm standard error of mean (SEM).

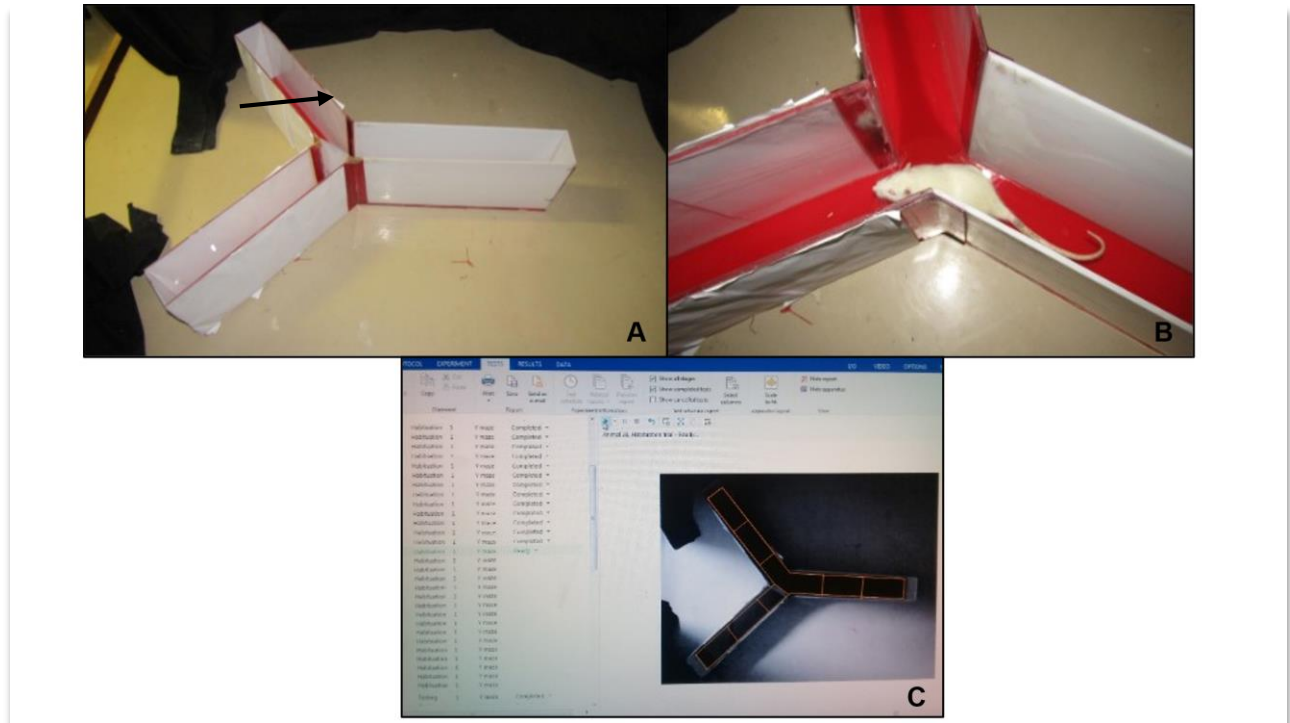


Figure 4.1 A.) The structure used for the Y-Maze. The arrow indicates the partition used to separate the novel arm of the maze. B.) An animal during the testing phase of the Y-Maze test. The partition of the novel arm has been removed to allow exploration C.) The use of the ANY-Maze software during the habituation phase of the Y maze behavioural test.

4.3 Results

Figures 4.2 illustrates the analysis of the Y-Maze behavioural test in adult male Sprague-Dawley rats, after exposure to LPS, and PBS in the case of the control group. Statistical analysis was conducted using the Graphpad Prism 8. All the animals were tested using the Y Maze test. The animals randomized in the PBS group were seen to have made more arm entries, when compared to the animals administered LPS, which was found to be a slightly statistically significant result ($t(6) = 2.2251$; $P \leq 0.05$).

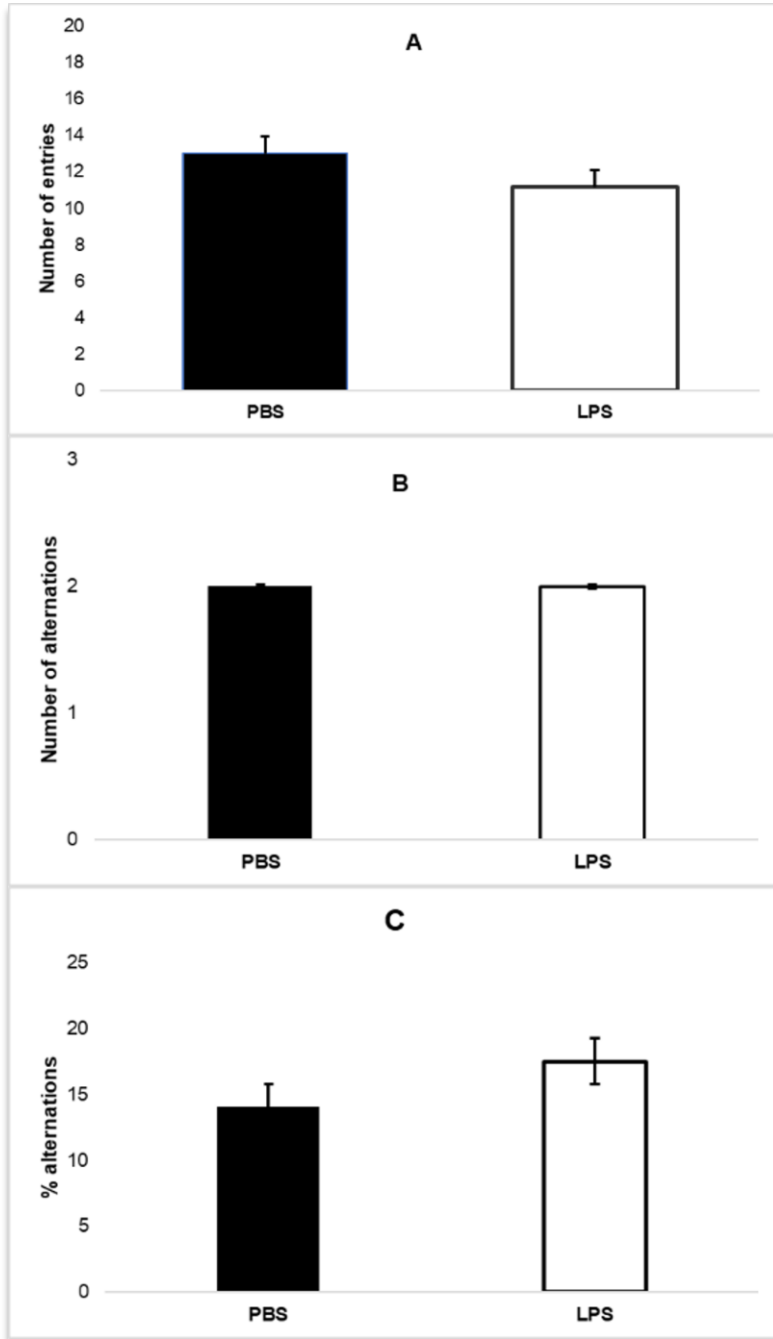


Figure 4.2 The effect of LPS administration on the spontaneous alternations in the y-maze in male Sprague-Dawley rats. The number of entries (A), the number of alternations (B) and the percentage of alternations (C). The Mean SEM = 3.58 (PBS) and 2.77 (LPS). * = $P \leq 0.05$

The animals that were administered LPS during the study period appeared to have made less alternations, but this decrease in the number of alternations as compared to the PBS group was not found to be statistically significant ($t(6)=0$; $P > 0.05$). While it appeared that the average

percentage of alternations was increased for the LPS in comparison to the PBS group, this result was not conserved to be statistically significant ($t(6) = 6$; $P > 0.05$).

4.4 Discussion

In the results obtained in this chapter, it was determined that the administration of PBS and LPS did not significantly alter or affect the short-term spatial memory of the animals tested in this study. One of the early symptoms of AD is the change in short-term memory³. Individuals affected by AD present with this symptom early in the disease's progression, which can be extrapolated in an aged population of Sprague-Dawley rats, as was attempted in this study⁵³. However, the fact that a shorter period of LPS administration was chosen for this study may have resulted in the animals' short-term spatial memory not to be affected to the degree expected in early-onset AD.

It was observed during the Y maze testing that the animals seemed more stressed than expected. The handling required during the administration phase of the study may have caused more stress than anticipated, despite the measures taken to decrease the effects of increased stress. These measures included testing during the animals' dark cycle, conducting a habituation period before testing and ensuring no white noise or outside factors would cause undue stress and anxiety in the animals, as advised by Prieur et al⁵⁰.

4.5 Conclusion

From the results obtained in the chapter, the administration of LPS in the animals did not alter the short-term spatial memory, as determined by the Y maze test. The low physiological concentrations of LPS administered (as outlined in Chapter 3) as well as the time of exposure did not have an impact on the animals as to be a representation of a sample population affected by AD.

Chapter Five

Investigating histological changes in the liver due to the effect of
LPS-induced inflammation by use of light microscopy

5.1 Chapter Objectives

To study the morphology of liver tissue damage, using light microscopy by Haematoxylin and eosin and Picrosirius red staining.

5.1.1 Introduction

In this chapter, the effects of LPS-induced inflammation on the liver of Sprague-Dawley rats were investigated, using light microscopy. The liver was chosen for analysis as it is one of the main organs involved in the immune response, serving as a buffer between the systemic circulation and gut-derived contents. The liver collects nutrients arriving from the gastrointestinal tract, through the portal vein. Toxins from intestinal bacteria are also cleared by the liver, highlighting its important detoxifying properties¹³. Normal liver histology, as seen when light microscopy is used for morphology analysis, will be described in this chapter, as well as the criteria used to determine instances where abnormal histology is seen as a result of systemic inflammation.

At a structural level, rat liver histology more closely resembles that of human liver, but there are some similarities to mouse liver. As in human liver, the hepatic microscope architecture can be described in the context of the classic liver lobules, which are polygonal structures that contain portal tracts, surrounding a central vein. Plates of hepatocytes, consisting of columns of hepatocytes that are 1 - 2 cells thick, extend from the portal region to the central vein, giving the appearance of these plates radiating away from the central vein⁵⁸⁻⁵⁹. Blood and bile circulate in opposite directions, with blood consisting of mixed arterial and portal venous blood moving from the portal region to the central vein via sinusoids. Sinusoids are the spaces that are seen between the hepatocyte plates. Hepatic portal regions across species are supported by stromal structures such as reticulin but may not be as apparent in rodents as in human liver, due to the smaller sizes of liver and the decreased amount of connective tissue⁵⁸. Located between the sinusoid and liver cells is the space of Disse, which contains plasma, connective tissue (mainly type III collagen), and hepatic stellate cells⁵⁹.

Inflammation causes changes to this normal microscopic architecture, particularly in the space of Disse and the hepatocyte plates. Portal hepatitis, where the limiting layer of hepatocytes is seen to expand outwards, is indicative of inflammatory injury. Systemic inflammation has also been

seen to affect the development of fibrosis, causing increased activity in hepatic stellate cells. This increased activity triggers extracellular matrix synthesis, leading to collagen fibre deposition in the spaces of Disse⁶⁰⁻⁶¹. However, in comparison to human liver, rat liver has much less discernible collagen and other connective tissue, and the bridging cords of collagen that extend between the portal regions and the central vein and nodular regeneration that are characteristic of liver fibrosis are seen to a less extent in rat liver. While staining sample slides with Haematoxylin and eosin (H&E) may show collagen formation in the portal regions, other stains such as Picrosirius red may be better able to detect and clearly show collagen formation in rat liver⁵⁸.

5.2 Materials and methods

5.2.1 List of reagents and materials used

- Mayer's Haematoxylin solution (Sigma-Aldrich)
- Eosin Y (Sigma-Aldrich)
- Picrosirius red stain (Sigma-Aldrich)
- Scott's Tap Water Substitute (Sigma-Aldrich)
- Glass vials, 10mL (Lasec)
- Formaldehyde solution (36.5 - 38% in H₂O; Sigma-Aldrich)
- PBS (Sigma-Aldrich)
- Ethanol (Sigma-Aldrich)
- Xylene (Sigma-Aldrich)
- Tert-butanol (ACS reagent, ≥ 99.0%; Sigma-Aldrich)
- Entellan mounting medium (Sigma-Aldrich)
- Coverslips and slides (Lasec)
- Pelleted wax (Sigma-Aldrich)
- White cassettes (Lasec)
- Microtome (Leica)
- Single edge blades (Biotech)
- Distilled water (ddH₂O) (Sigma-Aldrich)
- Zeiss Axio Imager.M2 (Zeiss, Germany)

5.2.2 Tissue extraction for light microscopy

Samples for light microscopy analysis were obtained as detailed in chapter 3.

5.2.3 Paraffin wax embedding with *tert-Butyl* alcohol

The process for embedding rat liver tissue samples for light microscopy is detailed in chapter 3, and has been adapted from Venter⁵¹. *Tert-Butyl* alcohol wax embedding was used instead of xylene, as previous evidence has shown that normal paraffin embedding with xylene results in irregular liver sample sectioning and inadequate tissue infiltration⁵¹.

5.2.4 Haematoxylin & Eosin staining

Haematoxylin and eosin (H&E) staining was done to evaluate any general structural changes that may have occurred because of the induced inflammation. For this, slides were rinsed in xylene to remove the paraffin wax, and then placed in a series of descending ethanol concentrations (100% twice, 90%, 70%) to rehydrate the tissue. The slides were placed in distilled water for 1 minute, and then placed in Haematoxylin for 10 minutes. After this, the slides were placed in Scott's buffer for 7 minutes, and then dipped into eosin. The slides were then placed in distilled water again for 1 minute, before being dipped into ascending concentrations of ethanol (70%, 90%, 100%), to dehydrate the samples and ensure that any excess dye has been removed. Finally, the slides were dipped in xylene, and mounted with entellen and coverslips. The slides were then viewed using a light microscope.

5.2.5 Picrosirius red staining

Picrosirius red staining was done to evaluate the formation and presence of collagen and/or fibrosis in the liver. For this to be achieved, the fixed slides were deparaffinized, then hydrated with descending concentrations of ethanol (100%, 95% and 70% ethanol). The slides were then stained with haematoxylin for 8 minutes, and washed for 10 minutes under running tap water. The slides were then stained with picrosirius red for one hour, after which they were washed twice with acidified water. Any excess water was physically removed by shaking the slides, before being further dehydrated three times in 100% ethanol, after which they were cleared in xylene, and

coverslips were mounted. The slides were viewed using a light microscope at a resolution of 100x magnification, under polarized light.

5.3 Results

5.3.1 Haematoxylin and eosin staining

The light micrographs of liver tissue samples of the control and experimental groups, stained with H&E, are shown in Figures 5.1 and 5.2. Figure 5.1 (A) is a representation of a sample from the control group, and shows the typical structural morphology of the rat liver portal region stained with H&E. Rat liver tissue tends to stain paler than human liver tissue, and the hepatocytes that extend from the portal regions are distinctly single cell, even at a low magnification. Slight portal hepatitis can be seen in the experimental group, as the limiting layer of the hepatocyte plate

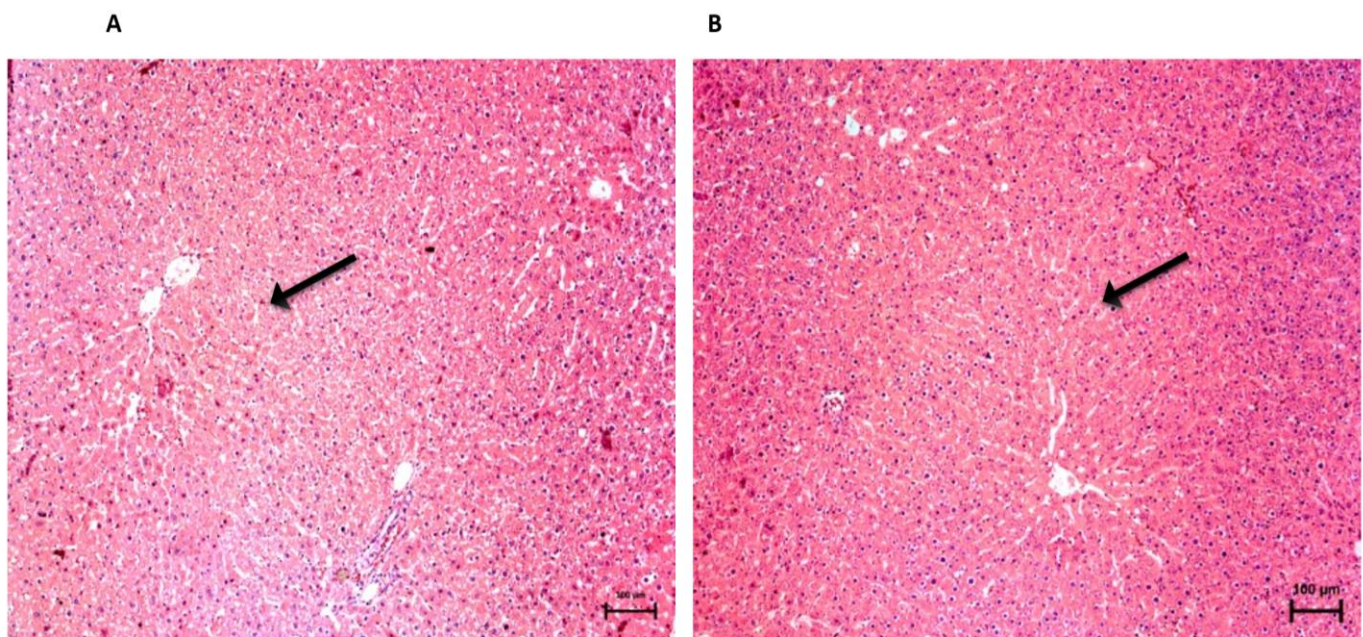


Figure 5.3 Light micrographs showing the microscopic architecture of rat liver tissue stained with H & E, of control (A) and experimental (B) groups. The portal triads or regions (black arrows) can be seen and are distinctly single-cell. Scale bar = 100 µm, visualized at 100x magnification.

seems slightly expanded.

Figure 5.2 represents the light micrographs of rat liver under a higher magnification, of the control group (A) and the experimental group (B) after exposure to LPS. Both the control and experimental groups show sinusoidal dilatation or ballooning, although it is present to milder effect in the control group. This sinusoidal dilatation, seen as white areas surrounding the hepatocyte nuclei, is indicative of inflammation in the liver⁵⁸.

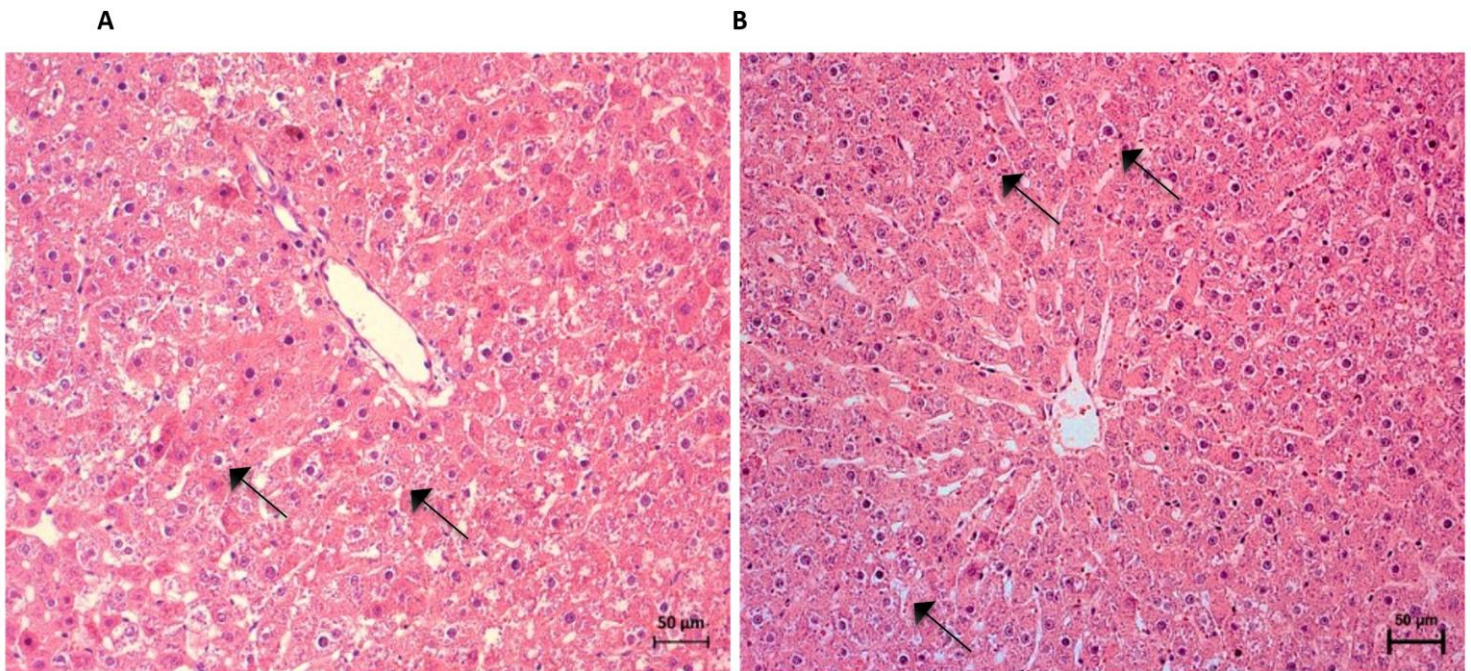


Figure 5.4 Light micrographs showing rat liver tissue stained with H&E of the control (A) and experimental(B) groups, visualized at a higher magnification (200x). The slight to moderate sinusoidal dilatation (white areas surrounding the nuclei) are indicated with black arrows. Scale bar = 50 μm

5.3.2 Picrosirius red staining

The light micrographs of liver tissue in the control and experimental groups are represented in figures 5.3 and 5.4. In figure 5.3 (A), the control group is represented, showing minimal collagen fibre deposition. Figure 5.3 (B) represents the experimental group, which shows minimal, but more marked collagen fibre deposition.

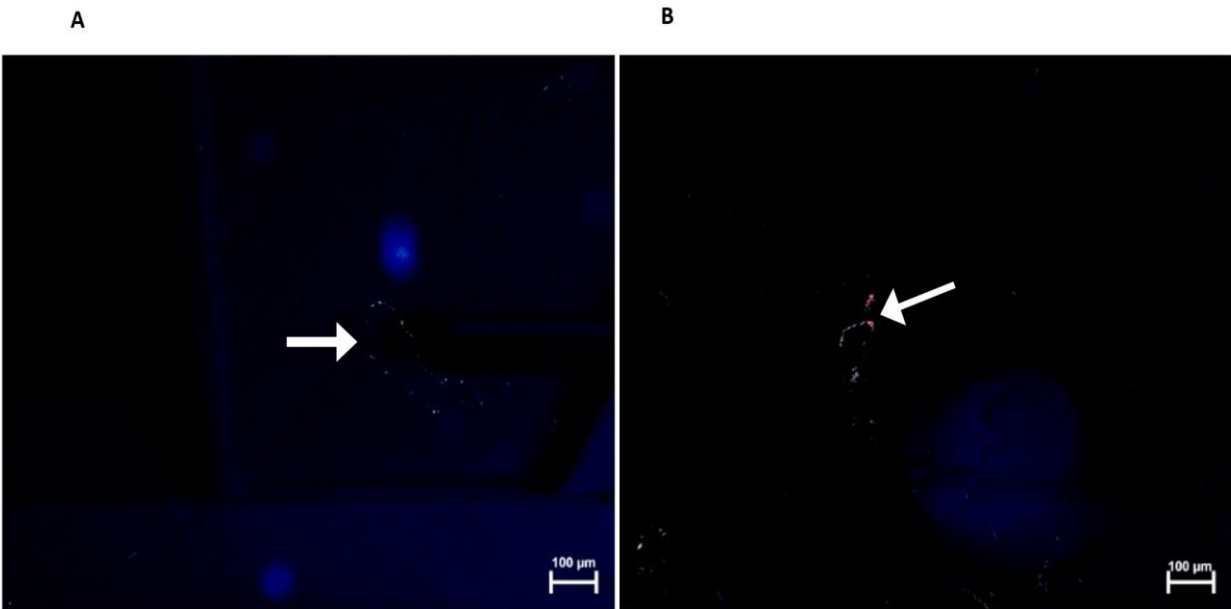


Figure 5.3 Polarized light micrographs of rat liver tissue samples in the control (A) group and experimental (B) group, stained with Picrosirius red. Fibrin fibres (stained red) are indicated with white arrows. Scale bar = 100 μm , visualized at 100x magnification.

Figure 5.4 represents a polarized light micrograph of liver tissue in the experimental group, taken from two different samples ($n = 2$). These micrographs show mild to moderate collagen fibre deposition, indicative of the progression of tissue damage due to LPS-induced inflammation. In

both the control and experimental groups, collagen fibre deposition was found near portal regions, particularly surrounding the blood vessels.

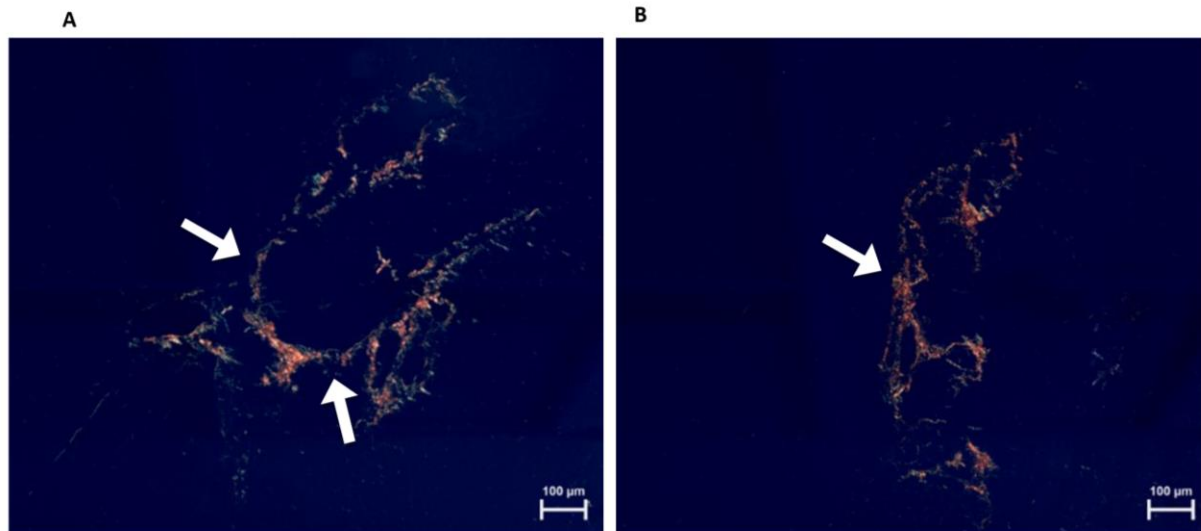


Figure 5.4 Polarized light micrographs of rat liver tissue samples in the experimental group (A and B) stained with Picrosirius red. The white arrows indicate areas of collagen fibre deposition, seen in orange-red. Scale bar = 100 µm.

5.4 Discussion

Alterations in the histology of liver tissue were observed in both the experimental and control groups, however the alterations found in the control group were minor. The control group exhibited mostly normal hepatic cord extension from the portal regions, as is typically seen in rat liver tissue histology under H&E staining⁵⁸.

In both the control and experimental group samples, sinusoidal dilation was found, which is a hallmark indicator of inflammation-induced fibrosis and cirrhosis^{62,63}. Figure 5.2 shows that in both the control and experimental groups, there is evidence of sinusoidal dilation. In the control group, this dilation is minimal, and may be due to the stress endured by the rats during the experimental phase of the study. The sinusoidal dilatation seen in the experimental group was more prevalent than in the control group, but did not indicate severe systemic inflammation. It may be that the period of LPS exposure was not extensive enough, and the results may indicate the early phase of systemic inflammation-induced liver damage⁶⁴.

Plates of hepatocytes are anchored by reticulin, as well as other collagen types, particularly Collagen Type III. However, rat liver tissue is known to contain lower levels of collagen fibres when compared to human liver, suggesting that the rate of collagen fibre deposition is less marked during inflammatory process. As was seen in this study, the presence of collagen fibre deposition was minimal to mild. This can also indicate that the concentration of LPS the animals were exposed to during the course of the study only elicited an early systemic inflammation response⁶⁴.

5.5 Conclusion

It can be said that LPS-induced inflammation causes changes to the way the liver resolves liver damage, in particular collagen fibre deposition, but the changes seen to the morphology of rat liver only indicate minimal to mild liver tissue damage, possibly indicative of the early stages of systemic inflammation. Future studies would have to look at a longer period of LPS exposure, at small concentrations, in order to find the changes associated with severe liver damage that can lead to cirrhosis.

Chapter Six

Investigating changes to liver cell ultrastructure due to the effect of LPS-induced inflammation by use of transmission electron microscopy

6.1 Objectives

The objective of this chapter is to outline the use of TEM in this study, the normal ultrastructure of liver cells as observed using TEM, as well as discuss the alterations to liver cell ultrastructure in a systemic inflammatory response.

6.1.1 Introduction

Liver fibrosis is a crucial process in the inflammatory response, and its resolution ensures continued homeostasis and a functional liver. A systemic inflammatory response has been shown to activate the pathological processes that result in organ dysfunction, such as persistent liver fibrosis (and decreased resolution), its evolution into cirrhosis and eventual liver failure^{13,19}. Organ dysfunction may also affect the liver's ability to produce proteins, particularly the coagulation factors that play an important in the initiation of the inflammatory response and the resolution of fibrosis.

While necrosis and apoptosis are known to be the main drivers of fibrosis, it has been suggested that there may be other mechanisms that may be the cause of organ failure in a systemic inflammatory response, due to some studies finding no discernible changes to normal organ appearance in an inflammatory response, despite the clear association between organ failure and LPS-induced systemic inflammation⁶⁵. The use of TEM may be useful in evaluating the changes to certain organelles and membranes of the different cells present in the liver.

Endoplasmic reticulum (ER) is an organelle present in most cells, and is responsible for protein folding and transport, lipid synthesis and calcium and redox homeostasis⁶⁶. It consists of the nuclear envelope and the peripheral ER, composed in a continuous membrane that includes flat, rough sheets and branched tubules. The rough sheets, known as rough ER due to an abundance of ribosomes present, are the main site for protein synthesis, protein folding and protein translation. Endoplasmic reticulum tubules are characterized by the presence of fewer ribosomes, and their smooth and curved surface. These tubules are known as smooth ER. Highly specialized cells, such as liver cells, are composed of ER largely made up of sheets, while cells with a higher content of tubules are those that are involved in processes such as lipid biosynthesis⁶⁷. Under normal conditions, the ER is in a state of equilibrium between its protein

load, and its capacity for folding⁶⁶. As such, it is an important organelle to consider for analysis, in terms of the liver's ability to produce coagulation factors needed for the acute inflammatory response.

Changes in ER homeostasis is a phenomenon known as ER stress, which may be the result of misfolded protein, increased protein synthesis and changes in the Ca²⁺/redox balance. Cells are equipped to deal with ER stress, through the unfolded protein response (UPR) pathway. This is an adapted pathway that re-establishes ER homeostasis in 2 ways, by either increasing folding capacity, or by down-regulation of the ER protein load through the inhibition of protein translocation and promotion of misfolded protein degradation⁶⁵.

Hepatocytes are known to have an abundance of ER, leading to the assumption that ER in the liver would be the key target of inflammatory mediators induced by LPS administration⁶⁸. Studies have shown that the development of ER stress can also initiate an inflammatory response; persistent ER stress may explain the occurrence of liver failure that can result from systemic inflammation without the appearance of necrosis or apoptosis⁶⁹. Therefore, changes to the ER present in hepatocytes will be of particular interest in this study, which may include narrowing of ER, absent ribosomes, or ER dilation⁶⁵.

Nuclei are found in the centre of most cells (excepting blood cells), are usually round or oval in shape and consist of a nuclear envelope, chromatin and the nucleolus. The nuclear envelope consists of a double membrane that fuses periodically to form nuclear pores to allow for metabolic exchange. Chromatin, the material that consists of DNA and histone proteins, appears as a cluster of small and dark granules and is important for the processes of DNA replication and cell division. Hepatocytes are known to sometimes contain more than one centrally located nucleus⁷⁰. In this study, changes to nuclear membrane integrity and the degree of chromatin condensation will be investigated as result of LPS-induced systemic inflammation.

6.2 Materials and methods

6.2.1 List of reagents and materials

- Glass vials, 10 mL (Lasec)

- Ethanol 99.5% (Sigma Aldrich)
- Glutaraldehyde solution, Grade I, 25% in H₂O, 50ml (Sigma Aldrich)
- Formaldehyde solution, 36.5-38% in H₂O , 500ml (Sigma Aldrich)
- Single edge blades (Advanced laboratory solutions)
- Osmium tetroxide solution, 4% in H₂O (Sigma Aldrich)
- PBS (Sigma Aldrich)
- Propylene oxide (Sigma Aldrich)
- Resin (Advanced laboratory solutions)
- JEOL JEM 2100F transmission electron microscope (JEOL USA Inc.)
- Sample grids (Advanced laboratory solutions)
- Uranyl acetate (Sigma Aldrich)
- Lead citrate (Sigma Aldrich)

6.2.2 Tissue extraction and fixation with 2.5% glutaraldehyde/formaldehyde

Samples for TEM analysis were obtained and fixated as detailed in chapter 3.

6.3 Results

The TEM micrographs of liver tissue in the control and experimental groups are represented in Figures 6.1. In Figure 6.1 A and C, the control group is represented, showing normal hepatocyte morphology, with each figure showing intact nuclei and nuclear membranes. Figure 6.1 B and D represent the experimental group exposed to LPS, showing moderate changes in the nuclear membrane. Figure D in particular, shows a view of an entire hepatocyte, and includes the presence of dilated endoplasmic reticulum, as well as showing the Space of Disse (dashed black arrow).

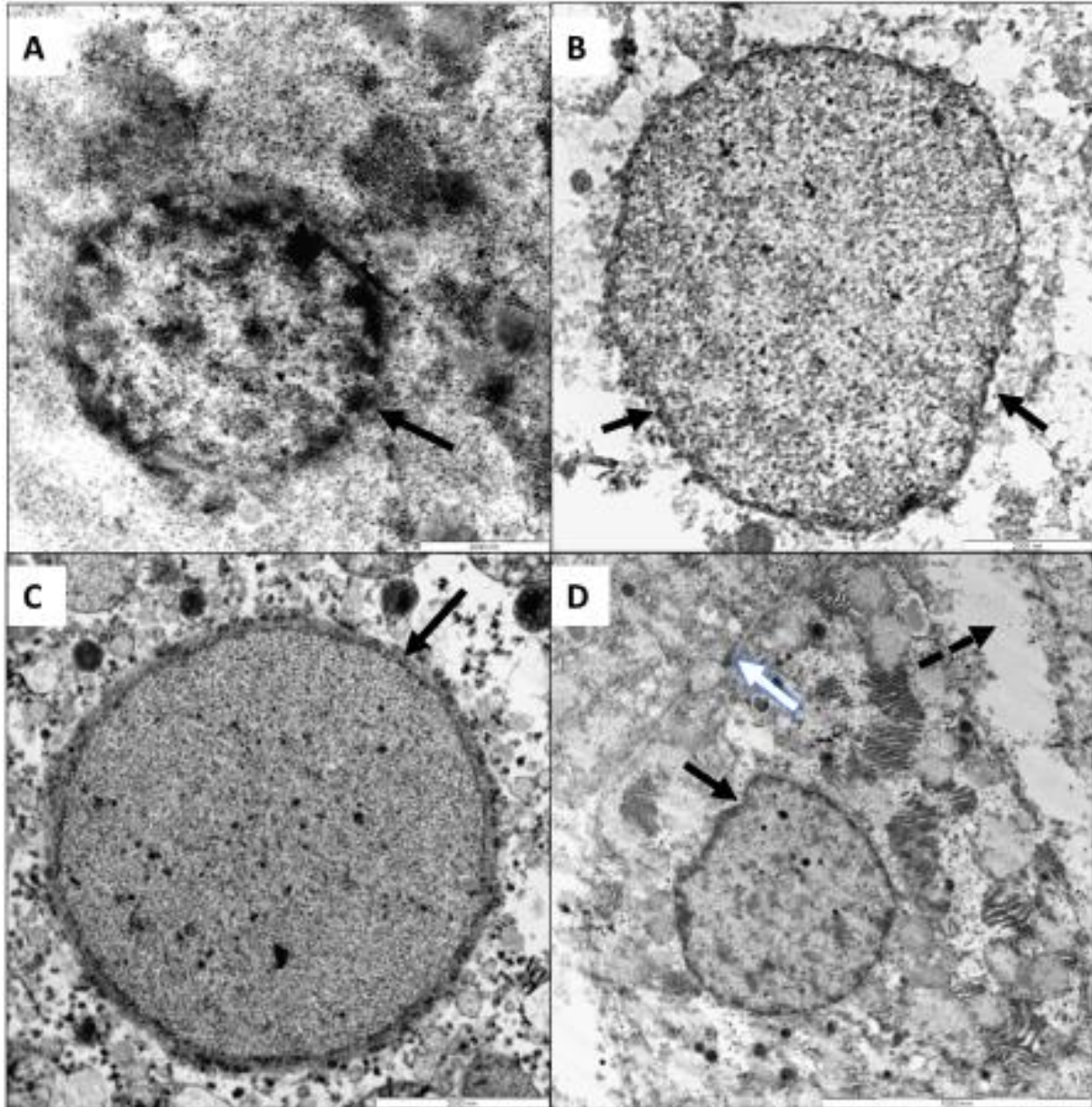


Figure 6.5 Transmission electron micrographs showing hepatocytes in liver tissue of control (A and C) and experimental (B and D) groups. The nuclei (solid black arrows) are prominent in A, B and C. D shows a view of an entire hepatocyte, including cell wall (white arrow with blue border), as well as the Space of Disse (dashed black arrow).

Figure 6.2 represents the transmission electron micrographs of hepatocytes in the liver tissue of the control group (A, B, and C) and the experimental group after exposure to LPS (D, E, and F). In all the figures, endoplasmic reticulum (solid black arrows) and the mitochondria can be seen. While the control figures show normal ER morphology, figures D, E, and F show dilated ER. In particular, the dilated ER seen in these figures seems to exhibit a smoother surface, indicating

the absence of ribosomes along the ER surface. The cisternae of the mitochondria cannot be clearly seen, with the mitochondria in figures A, B and C showing normal morphology. The

mitochondria in figures D, E, and F seem slightly enlarged, indicating some matrix swelling, and show minimal membrane disruption.

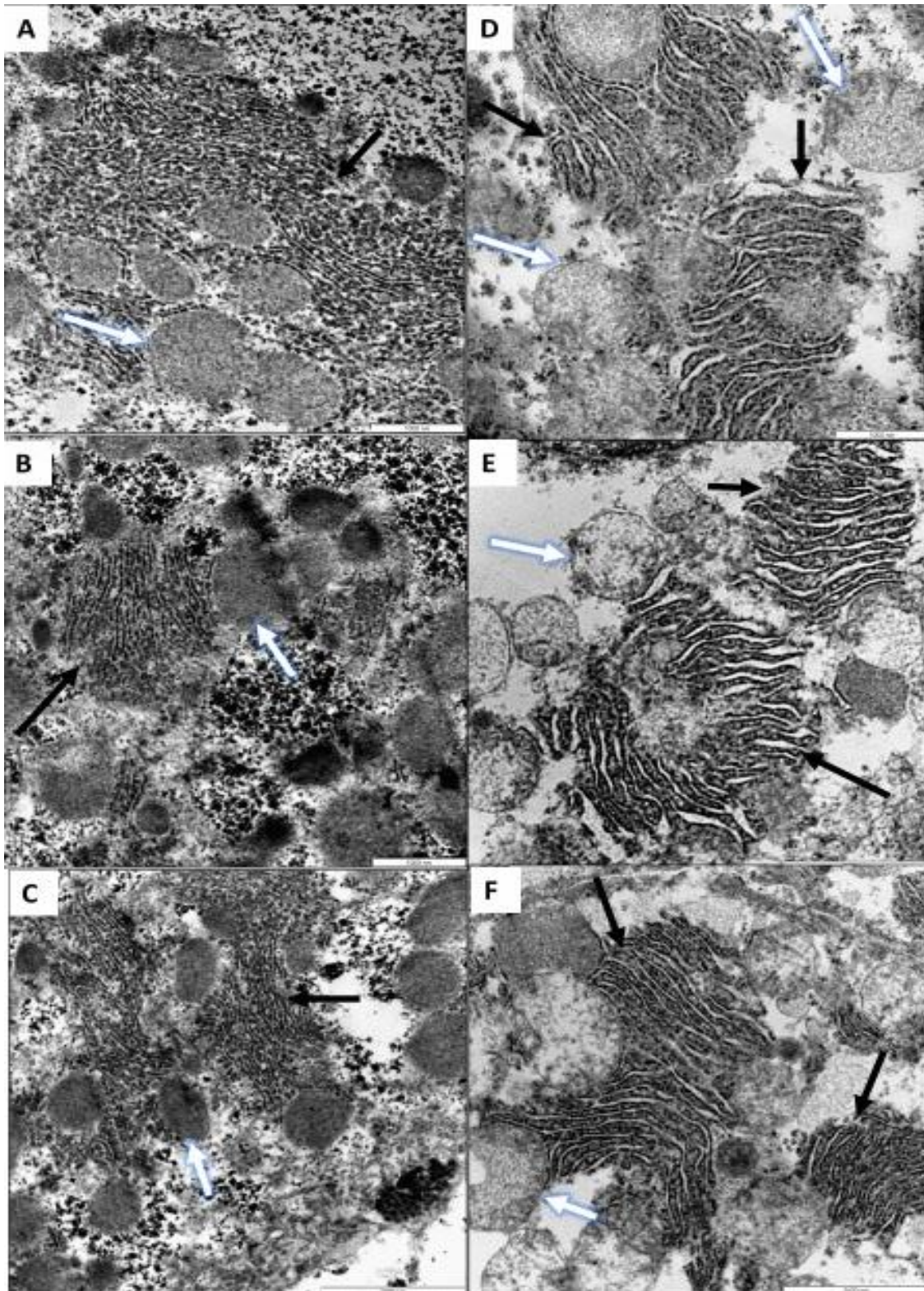


Figure 6.6 Transmission micrographs of liver tissue in the control (A, B, and C) and experimental (D, E, and F) groups. Mitochondria (white arrows, blue borders) and endoplasmic reticulum (solid black arrows) are shown.

Figure 6.3 represents the TEM micrographs of the Space of Disse in liver tissue in the control group (F) and the experimental group (A, B, C, D, and E). In figures A to E, moderate collagen fibre deposition can be seen indicating collagenisation of the Space of Disse. Hepatic stellate cells can also be seen in close proximity to the collagen fibre bundles, indicating that this collagen deposition is occurring in the Space of Disse. Furthermore, in the samples where collagen fibre deposition was seen, there was significant widening of the Space of Disse, which has been shown to occur when collagenisation takes place⁶⁸. Figure F represents the few collagen fibrils present in the Space of Disse in one sample of the control group; a larger representation of collagen fibres could not be in the control, as the other samples that were analysed were found to contain little to no trace of collagen fibres. This finding is consistent with the view that rat liver tissue express low levels of collagen, even under an inflammatory response.

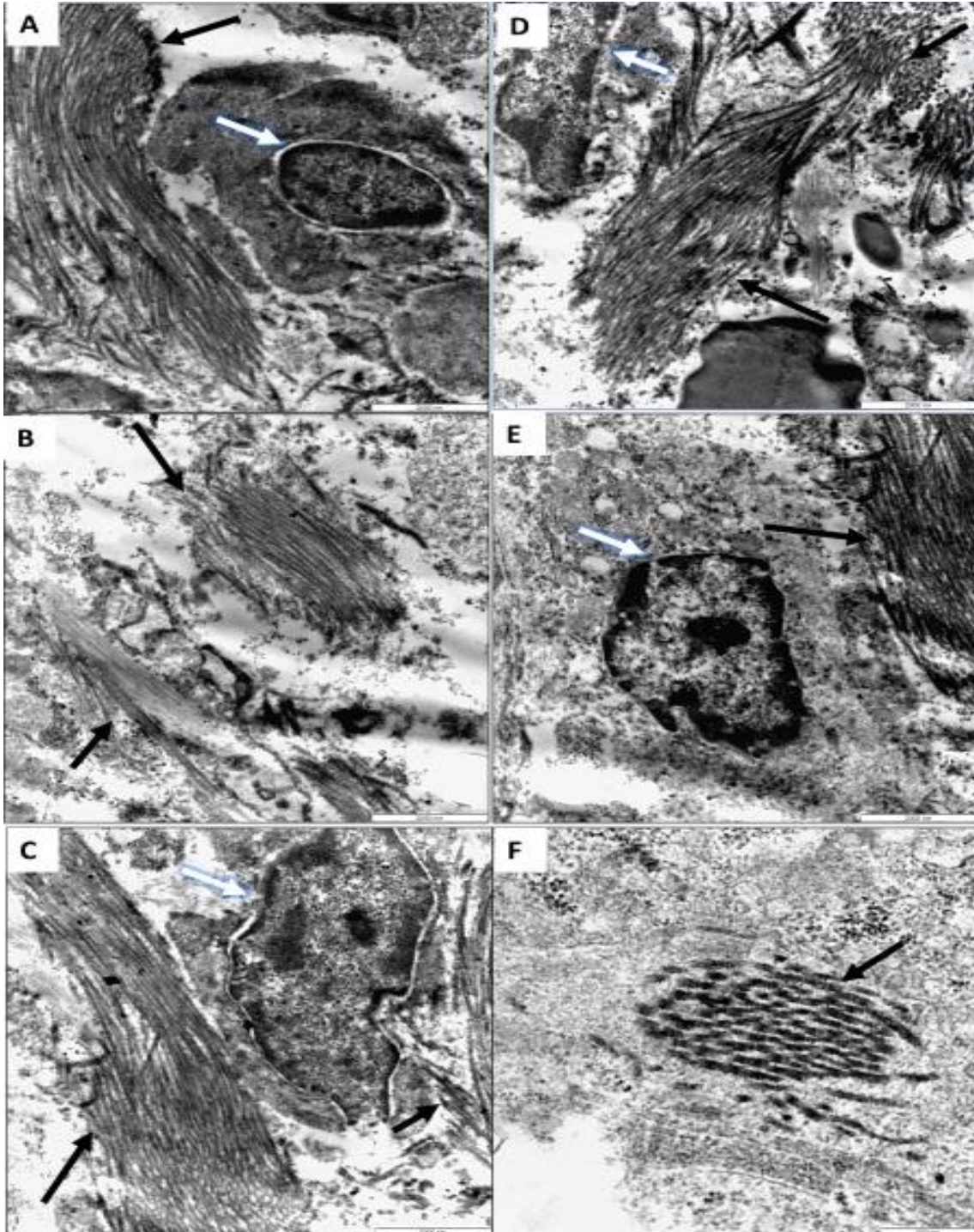


Figure 6.7 Figures A, B, C, D, and E are transmission electron micrographs of liver tissue in the experimental group, while figure F is a transmission electron micrograph of liver tissue in the control group. (Scale bars: A: 2000 nm; B: 2000 nm; C: 2000 nm; D: 2000 nm; E: 2000 nm; F: 500 nm)

Table 6.1 summarises the ultrastructural changes seen in liver tissue, and was used as a means to determine the severity of the overall damage that may have occurred as a result of LPS-induced inflammation.

Table 6.1: A summary of the ultrastructural changes in rat liver tissue

Group	General cell morphology	Cellular membrane disruption	Nuclear membrane disruption	Chromatin condensation	Endoplasmic reticulum dilation	Absence of ribosomes	Endoplasmic reticulum narrowing	Collagen fibre deposition
Control	+	-	-	-	+	-	+	-
LPS	++	+	++	+	+++	+	++	++

no change = -; mild = +; moderate = ++; severe = +++

6.4 Discussion

Liver fibrosis is a crucial part of the inflammatory response, and its resolution ensures the continued homeostasis and functionality of the liver. Systemic inflammation can disrupt this process, leading to organ dysfunction and, ultimately, liver failure. In this chapter, the effects of LPS administration on the liver's functionality as it pertains to coagulation factor production was evaluated in liver tissue by use of TEM. Of particular interest was the organelle most directly involved in coagulation factor production, endoplasmic reticulum. Other organelles that were also evaluated for possible alterations in their structure and morphology included the nuclear and cellular membranes, the mitochondria and collagen fibres.

Normal hepatocyte was observed in the control group (Figure 6.1 A and C; Figure 6.2 A, B, and C; Figure 6.3 F). In the experimental group that received LPS injections, there were indications of mild to moderate indications of tissue damage, with some samples showing more moderate to severe indications of liver damage (Figure 6.1 B and D; Figure 6.2 D, E and F; Figure 6.3 A-E). This damage was mostly seen in changes to the ER, some cellular and nuclear membrane disruption, as well as visible collagen fibre deposition and hepatic stellate cell activation. Of particular interest was the ER dilation that was seen in the experimental group, as compared to the ER in the control group. Similar changes were also reported in a study by Kozlov et al., in 2009, where the authors found that endotoxin (or LPS) resulted in ER dysfunctionality, characterized by ER dilation⁷¹. While not the focus of this study, the mitochondria in the experimental group were found to exhibit some slight changes after LPS administration, as compared to the control group. The mitochondria were also found to occur in close proximity to the dilated ER, indicating that mitochondrial function may be affected by LPS and could involve the ER. This was a similar finding to Kozlov et al., where the authors that hypothesised mitochondrial reactive oxygen species generation could lead to impaired ER function by way of the induction of ER stress and the UPR pathway⁷¹.

One change that was not anticipated, particularly in the early stages of the inflammatory response, was the deposition of collagen in the Space of Disse that was seen in some of the samples of the experimental group (n=3). This collagen deposition was seen to occur in conjunction with apparent hepatic stellate cell activation, which usually occurs during an inflammatory response⁷². This activation of hepatic stellate is of particular importance, as it one of the cell types that is thought to be involved in the incidence of fibrogenesis (along with myfibroblasts)⁷³.

6.5 Conclusion

From the ultrastructural findings of this chapter, it can be concluded that LPS administration in order to elicit an inflammatory response had a mild to moderate effect on the ultrastructure of the liver, a clear indication of the initial phases of the inflammatory response. These results indicate that although the period of LPS administration conducted in this study only resulted in the initial stages of the inflammatory response, it still had made a significant impact on the ability of endoplasmic reticulum to maintain optimum function, a further indication of ER stress. It must be noted, however, that there was no discernible or significant signs of necrosis or apoptosis; this may explain the occurrence of liver damage without the occurrence of significant cell death.

In conjunction with the development of ER stress, there were also ultrastructural changes to the Spaces of Disse, which was shown to have widened as result of hepatic stellate cell activation and collagenisation of the Spaces. It may be that continued induction of the inflammatory response due to LPS or endotoxin could result in further collagenisation, which can cause the liver to lose the state of homeostasis and result in liver damage.

Chapter Seven

Investigating changes in the levels of tissue factor and fibrinogen in the liver due to the effect of LPS-induced inflammation by use of Enzyme-linked Immunosorbent Assay

7.1 Chapter Objectives

The objective of this chapter is to determine the concentration of the coagulation factors, TF and fibrinogen, by use of ELISA assays.

7.1.1 Introduction

Tissue factor, a transmembrane receptor for Factor VII/VIIa, is considered as a major initiator of the coagulation cascade and has been shown to be a key link connecting coagulation, inflammation and immunological processes. It is expressed by cells surrounding blood vessels, as well as monocytes, particularly within hepatocytes that are in close proximity to portal regions. Extravascular TF is not freely circulating in cells, due to its separation from FVII by an endothelium, preventing inappropriate activation of the clotting cascade⁷⁴.

The liver usually expresses low levels of TF, monocytes found within hepatocytes that have been stimulated by LPS exposure are known to activate inflammatory mediators such as toll-like receptor 4 (TLR-4), leading to increased TF expression⁷⁵. This increased expression has been shown to induce high levels of TF expression, which leads to accumulation of TF in the liver, persistent activation of inflammatory mediators and liver damage. Despite these findings, models that have attempted to elucidate the link between TF expression and the development of hypercoagulation have ignored tissue or cells that traditionally express low levels of TF, as is the case with hepatocytes⁷⁶. However, it has been suggested that the activation of coagulation does not necessarily have to be a consequence of increased TF expression; rather, activation of the coagulation cascade could occur via molecular activation of the existing TF/FVIIa complex⁷⁶. This study aimed to induce systemic inflammation by exposure to LPS, it would therefore be expected that TF levels would be elevated in liver tissue.

The mechanisms surrounding the initiation of coagulation are still not clearly understood, but the idea that TF in the liver is expressed by hepatocytes and that hepatocyte TF is the main driver of coagulation activation in chronic liver disease has been established^{77,78}. The nature of liver sinusoids, with the mix of arterial and portal venous blood and its exposure to blood-borne pathogens, poses a serious challenge in the maintenance of haemostasis in the liver^{78,79}. There is evidence that disruption in the synthesis or expression of anticoagulant factors involved in the generation of fibrin can lead to its deposition and result in fibrosis⁸⁰.

The conversion of fibrinogen into fibrin is a crucial step in coagulation cascade, and the increase of fibrinogen is considered an indicator of an inflammatory state. This makes fibrinogen an important marker in the development of liver pathogenesis due to systemic inflammation. Lipopolysaccharide administration has been shown to influence thrombin expression, which in turn leads to increased fibrinogen expression, fibrogenesis and hepatic deposition. It has also been shown that the impaired removal of fibrin, as a result of a suppressed fibrinolytic system, contributes to fibrin deposition^{81,36}. Increased levels of fibrinogen are shown to be a feature of the HC state found in patients with AD⁴¹, therefore for this study, the levels of fibrinogen in liver tissue will be evaluated using ELISA, in order to determine if LPS-induced systemic inflammation contributes to an increase in fibrinogen.

7.2 Methods and materials

7.2.1 List of reagents and materials

- Rat FG(Fibrinogen) ELISA Kit, Catalog number: E-EL-R1125 (Elabscience Biotechnology Inc., USA)
- Rat TF(Tissue Factor) ELISA Kit, Catalog number: E-EL-R0984 (Elabscience Biotechnology Inc., USA)
- Microcentrifuge tubes (Lasec)
- Pipette tips (Lasec)
- Pasteur pipettes (Lasec)

7.2.2 Tissue extraction for ELISA testing

Samples for ELISA analysis was obtained as detailed in chapter 3.

7.2.3 Detection of tissue factor and fibrinogen levels in liver tissue

Detection of the levels of TF and fibrinogen in homogenized liver tissue samples were done using the Rat TF ELISA kit and the Rat Fibrinogen ELISA kit. For both assays, each protocol in the manual was followed. Each assay was done based on the sandwich-ELISA principle, where the micro-plate wells are pre-coated with a primary antibody specific to TF and fibrinogen.

A standard working solution was constituted and 100 μl was added to the first two columns of each well on the micro-plate. Each known standard is placed in duplicate wells, side by side. Then, 100 μl of the liver tissue samples were pipetted into each duplicate microplate well, as was done with the standard working solution, and incubated for 90 minutes at 37°C. Any TF/FVII or FG present is bound by the immobilised antibody. After incubation, the liquids were removed from each well, and biotin-conjugated antibody specific to each TF and fibrinogen was immediately added to each well. The plate was covered with a plate sealer and incubated for 1 hour at 37°C. After the solution from each was aspirated, 350 μl of a wash buffer was added to each well, to remove any unbound or free components. After being allowed to soak for 2 minutes, the solution was aspirated from each and the plate was patted against absorbent paper to dry. This wash was repeated 3 times. After the wash, 100 μl of a conjugate working solution of avidin-Horseradish Peroxidase (HRP) was added to each well, covered with a plate sealer and incubated for 30 minutes at 37°C. The solution in the wells was then aspirated, after which a second wash process was repeated as conducted earlier, this time for five times. Then, 90 μl of the substrate reagent was added to each well; the plate was covered with a plate sealer and incubated for 15 minutes 37°C. This substrate allows for a colour change reaction to occur, if there is any TF or fibrinogen present in the well. After incubation, 50 μl of a stop solution was added to each well. The above procedure was performed in triplicate. The micro-plate was placed in a microplate reader (Labotec (Pty) Ltd.). The optical density of each sample was measured with a microplate reader at wavelength of 450 nm.

The unknown concentration of each sample was calculated by use of a logistic curve, with the standard concentration on the x-axis and the optical density values on the y-axis. The unknown concentrations were determined by extrapolating the optical density measured by the plate reader onto the x-axis.

7.3 Statistical analysis

Statistical analysis was performed using the Mann Whitney U test (also known as the Wilcoxon rank-sum test). P values less than 0.05 were considered statistically significant.

7.4 Results

The results from the both the TF and fibrinogen ELISA assays can be seen in Figure 7.1 and 7.2.

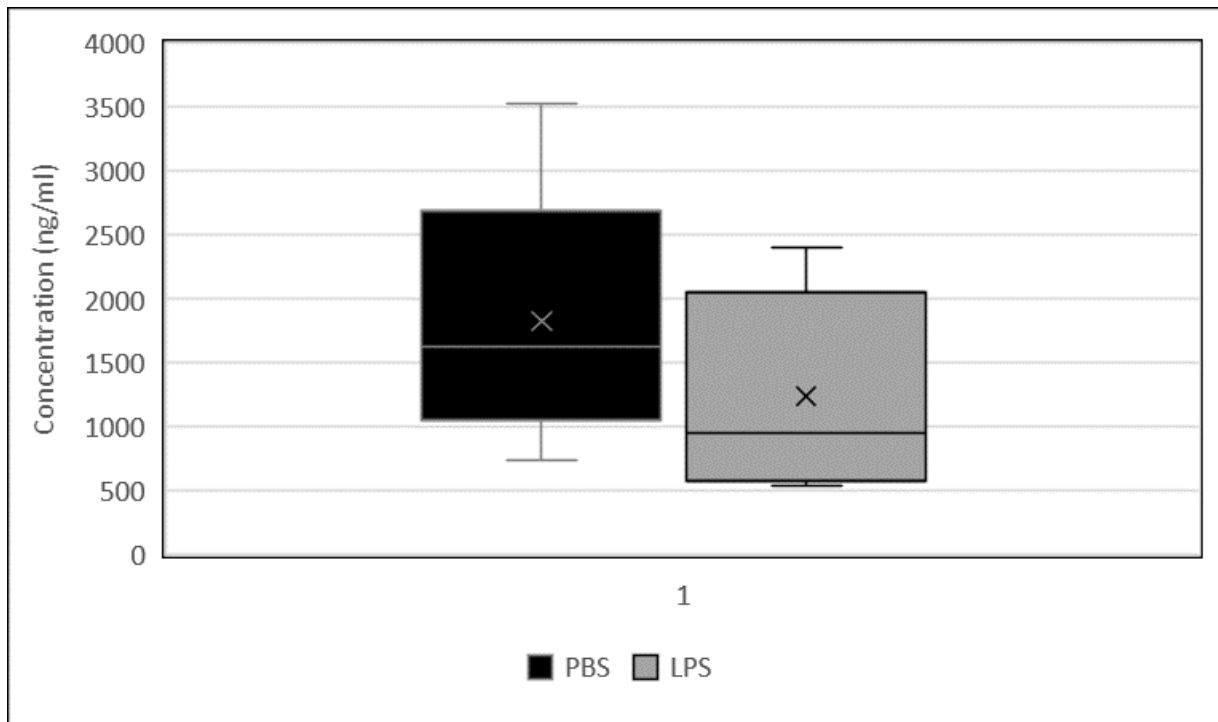


Figure 7.8 Box plot showing the distribution of tissue factor concentration between the control and experimental groups

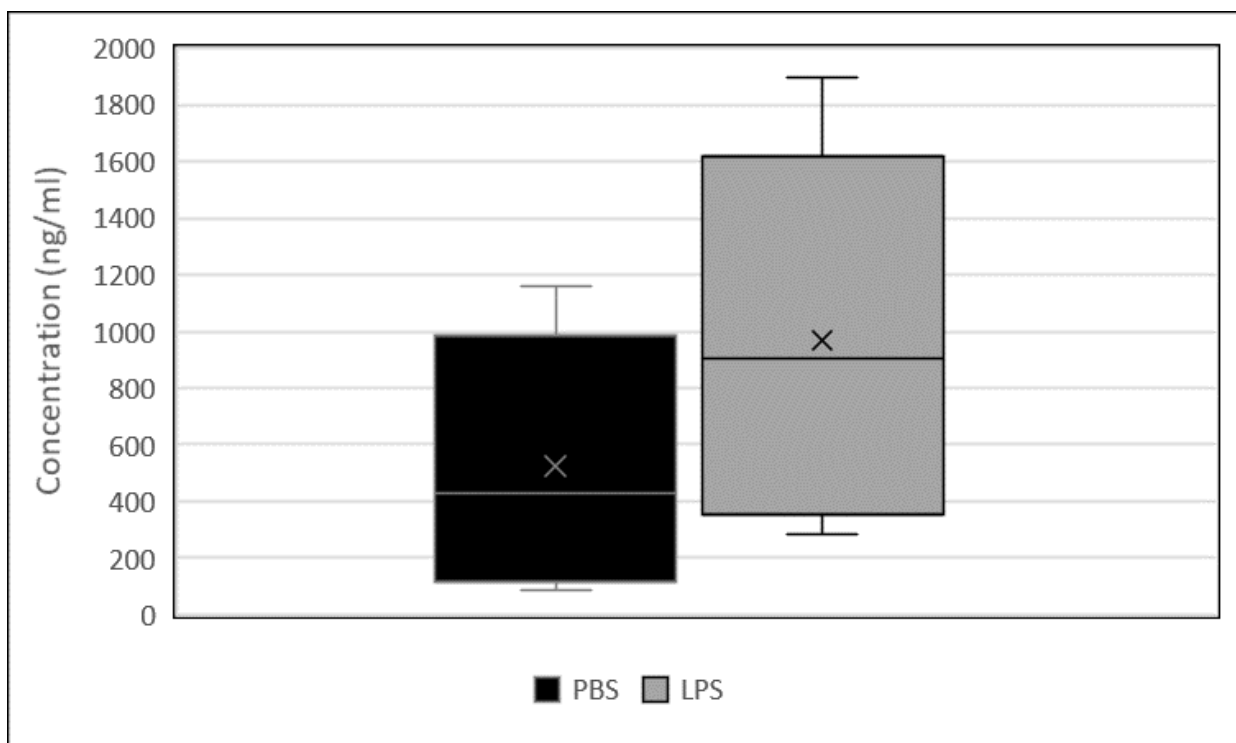


Figure 7.9 Box plot showing the distribution of fibrinogen concentration between the control and experimental groups

In this chapter the control group was compared against the experimental group to determine if they were statistically different for TF concentration levels in rat liver after LPS exposure. No statistical difference was found between the control and experimental groups, (P value = 0.8534; Figure 7.1). For fibrinogen concentration levels after LPS exposure, it was found that there was no statistical difference (P value = 0.7394) between the control and experimental groups (Figure 7.2).

7.5 Discussion

Tissue factor is known to be prevalent at low levels in hepatocytes⁷⁶, which seemed to be the case in both the experimental and control groups studied. Tissue factor expression in hepatocytes has been suggested to be the main proponent of procoagulant activity in the liver. It has also been suggested that TF expression does not necessarily have to be increased to induce the inflammatory cascade, it may be that inflammation causes molecular activation of existing TF in hepatocytes^{76, 78}.

In the result obtained in this chapter, the levels of fibrinogen were not significantly different in between the control and experimental groups; that is, there was no significant increase in the concentration levels of fibrinogen after LPS exposure, as would be expected during systemic inflammation. It can be deduced that the LPS exposure the animals were subjected during the course of the study did not induce a hypercoagulable state, as there does not seem to have been a marked increase in fibrinogen levels, an indicator of the inflammatory state⁸¹.

The statistically insignificant results of this study obtained in this study may be due to the fact that the concentration of LPS the animals were exposed to were of smaller quantities and a shorter response time, compared with other studies that used a single dose model, as executed by Lee et al.⁸².

7.6 Conclusion

It can be concluded that the LPS exposure carried out in this study did not cause a change in the production of the TF and fibrinogen levels during low levels of LPS exposure.

Chapter Eight

Conclusion

There have been significant strides made in AD research, particularly the establishment of the core pathologies of the disease: amyloid- β plaque formation, hyperphosphorylation of tau protein and neuronal cell death that causes dementia. Despite this, there still remains limited understanding of precisely how these pathologies initially developed, due to the fact that they develop over a prolonged period, manifesting in the dementia symptoms that develop later in life. This has resulted in the well-documented difficulties in developing effective treatment of AD.

In recent years, the idea of AD being an inflammatory disease has taken hold and AD is now considered to be inflammatory disease. However, significant numbers of those diagnosed with AD will have died from an acute secondary illness, such as cardiovascular or respiratory illnesses. Due to the long progression of AD pathogenesis, systemic inflammation has become the major focus of research. Lipopolysaccharide has been used extensively in research to induce systemic inflammation in attempt to mimic to the pathogenesis of AD. The liver would be the first organ to be exposed to the effects of LPS, as it is an important buffer between the gut and systemic circulation, known as the gut-liver axis. Due to its many functions, particularly its role in the regulation of factors involved innate immunity, the liver is considered an immunological organ.

In this study, the effects of LPS-induced inflammation were investigated in the livers of adult male Sprague-Dawley rats, with particular focus on the liver's morphology and function in the production of coagulation factors. This model has been widely used to recreate the inflammation seen in neurodegenerative diseases. This study investigated the effects of LPS-induced inflammation on liver tissue by use of light microscopy and TEM, along with the analysis of the coagulation factors TF and fibrinogen by use of the ELISA assays. The LPS model was implemented over a 10 day experimental period, which also included the use of behavioural testing to confirm the spatial memory deficits that occur as a result of exposure to LPS, as outlined in chapter 4.

The histological and ultrastructural changes in the liver tissue of the animals after LPS administration were investigated in comparison to the liver tissue of the rats in the control group. There were specific criteria that were used to determine if the administration of LPS had any effects on the morphology and organelle structure of liver tissue. These criteria included changes to hepatic portal vein architecture, with particular focus on the sinusoid and spaces of Disse; the development of endoplasmic reticulum stress through the dilation of the endoplasmic reticulum and collagen fibre deposition. The examination of liver tissue using

these criteria as a result of LPS administration yielded mild to moderate changes in the histology and ultrastructure, indicating that the low-grade inflammation induced by the low concentration of the administered LPS may have only resulted in the initial stages of liver damage^{62-64, 71-72}.

This determination was further corroborated by the results from the TF and fibrinogen levels that showed no changes in the animals exposed to LPS when compared to the control group. Therefore, it appears that the function of the liver by producing coagulation factors have not yet been affected.

The outcome of this model indicates that low levels of LPS exposed short term may contribute to ER stress in liver cells. This could potentially accumulate during long term exposure and this might lead to clinical presentation. Future studies could implement an increased concentration or dosage of LPS, administered over a longer period that may induce the kind of behavioural and morphological changes that would be expected in the development of liver damage and subsequent fibrosis. In addition, it was observed that the age of the animals used for this study may have contributed to the results obtained. While the use of Sprague-Dawley rats in models studying the pathogenesis of neurodegenerative disease has been well-established, it may be recommended to use animals that are more aged than the sample population used for this study, therein ensuring that the animals are a closer representation of the typical population of those diagnosed with AD.

References

1. Alzheimer's Association Report. 2020 Alzheimer's disease facts and figures. *Alzheimer's Dement.* 2020; 16: 391-460
2. Kinney JW, Bemiller SM, Murtishaw AS, Leisgang AM, Salazar AM & Lamb BT. Inflammation as a central mechanism in Alzheimer's disease. *Alzheimer's Dement.* 2018; 4: 575-590
3. Bolós M, Perea JR & Avila, J. Alzheimer's disease as an inflammatory disease. *Biomol Concepts.* 2017 Mar 1;8(1):37-43
4. Zhang F & Jiang L. Neuroinflammation in Alzheimer's disease. *Neuropsych Dis Treat.* 2015 Jan 30; 11: 243–256
5. Kitazawa M, Oddo S, Yamasaki TR, Green KN & LaFerla FM. Lipopolysaccharide-induced inflammation exacerbates pathology by a cyclin-dependent kinase 5-mediated pathway in a transgenic model of Alzheimer's disease. *J Neurosci.* 2005 September 28; 25(39): 8843-8853
6. Cortes-Canteli M, Zamolodchikov D, Ahn HJ, Strickland S, Norris EH. Fibrinogen and altered hemostasis in Alzheimer's disease. *J Alzheimer's Dis.* 2012 January 1; 32(3): 599-608
7. Raetz CRH & Whitfield C. Lipopolysaccharide endotoxins. *Annu Rev Biochem.* 2002; 71:635-700
8. Alexander C, Rietschel ET. Bacterial lipopolysaccharides and innate immunity. *J Endotoxin Res.* 2001 January; 7(3): 167-202
9. Andreasen AS, Krabbe KS, Krogh-Madsen R, Taudorf S, Pederson BK, Moller K. Human endotoxemia as a model of systemic inflammation. *Curr Med Chem.* 2008; 15: 1697-1705
10. Asti A. Bacterial lipopolysaccharide (LPS) and Alzheimer's disease. In Miklossy J, editor. *Handbook of infection and Alzheimer's disease.* IOS Press. 2017: p. 383-394
11. Nolan JP. The role of intestinal endotoxin in liver injury: a long and evolving history. *Hep.* 2010 August 6; 52(5):1829-35
12. Anders H-J, Andersen K & Stecher B. The intestinal microbiota, a leaky gut, and abnormal immunity in kidney disease. *Kidney Int.* 2013 January 16; 83: 1010-1016
13. Brandl K & Schnabl B. Is intestinal inflammation linking dysbiosis to gut barrier dysfunction during liver disease? *Expert Rev Gastroenterol Hepatol.* 2015; 9(8): 1069-1076
14. Robinson MW, Harmon C, O'Farrelly C. Liver immunology and its role in inflammation and homeostasis. *Cell Mol Immunol.* 2016 April 11; 13: 267-276

15. Mimura, Y., Sakisaka, S., Harada, M., Sata, M. & Tanikawa, K. Role of hepatocytes in direct clearance of lipopolysaccharide in rats. *Gastroenterol.* 1995 July 28. 109: 1969-1976
16. Shetty S, Lalor PF, Adams DH. Liver sinusoidal endothelial cells – gatekeepers of hepatic immunity. *Nat Rev Gastroenterol Immunol.* 2018; 15: 555-567
17. Knolle PA, Wohlleber D. Immunological functions of liver sinusoidal endothelial cells. *Cell Mol Immunol.* 2016 May; 13(3): 347-353
18. Knolle PA, Loser E, Protzer U, Duchmann R, Schmitt E, Zum Bushenfelde K-H M, Rose-John S, Gerken G. Regulation of endotoxin induced IL-6 production in liver sinusoidal endothelial cells and kupffer cells by IL-10. *Clin Exp Immunol.* 1997; 107: 555-561
19. Pellicoro A, Ramchandran P, Iredale JP, Fallowfield JA. Liver fibrosis and repair: immune regulation of wound healing in a solid organ. *Nat Rev Immunol.* 2014 March; 14(3): 181-94
20. Hoffman M. A cell-based model of coagulation and the role of factor VIIa. *Blood Reviews.* 2003; 17: S1-S5
21. Hoffman M & Monroe DM. A cell-based model of hemostasis. *Thromb Haemost.* 2001; 85: 958-965
22. Hoffman M. Remodeling the coagulation cascade. *Journal of Thrombosis and Thrombolysis.* 2003; 16(1/2): 17-20
23. Smith SA. The cell-based model of coagulation. *J Vet Emerg Crit Care.* 2009; 19(1): 3-10
24. Malato Y, Naqvi S, Schurmann N, Ng R, Wang B, Zape J, Kay MA, Grimm D, Willenbring H. Fate tracing of hepatocytes in mouse liver homeostasis and regeneration. *J Clin Invest.* 2011 December; 121(2): 4850-60
25. Forkin KT, Colquhoun DA, Nemergut EC & Huffmyer JL. The coagulation profile of end-stage liver disease and considerations for intraoperative management. *Anesth Analg.* 2018 January; 126(1):46-61
26. Levi M & van der Poll T. Coagulation in patients with severe sepsis. *Semin Thromb Hemost.* 2015; 41:9-15
27. Ilesanmi OO. Pathological basis of symptoms and crises in sickle cell disorder: implications for counseling and psychotherapy. *Hematol Rep.* 2010 Jan 26; 2(1):e2
28. Abshire TC & Jobe SM. Overview of the coagulation system. In: Shaz BH, Hillyer CD, Roshal M, Abrams CS, editors. *Transfusion medicine and hemostasis.* Elsevier Science; 2013. P. 587-592
29. Levi M, van der Poll, Buller HR. Bidirectional relation between inflammation and coagulation. *Circulation.* 2004 June 8; 109(22): 2698-2704

30. Vine AK. Recent advances in haemostasis and thrombosis. *Retina*. 2009 January; 29(1): 1-7
31. Mackman N. The many faces of tissue factor. *J Thromb Haemost*. 2009; 7(suppl. 1): 136-139
32. Franco RF, Jonge E, Dekkers PE, Timmerman JJ, Spek A, van Deventer SJH, et al. The in vivo kinetics of tissue factor messenger RNA expression during human endotoxemia: relationship with activation of coagulation. *Blood*. 200; 96: 554-559
33. Grover SP, Mackman, N. Tissue factor: an essential mediator of homeostasis and trigger of thrombosis. *Arterioscler Thromb Vasc Biol*. 2018; 38: 709-725
34. Davalos D, Akassoglou K. Fibrinogen as a key regulator of inflammation in disease. *Semin Immunopathol*. 2012; 34: 43-62
35. Anstee QM, Dhar A, Thursz MR. The role of hypercoagulability in liver fibrosis. *Clin Res Hepatol Gastroenterol*. 14 May 2011; 35: 526-533
36. Kopec AK, Luyendyk JP. Roles of fibrin(ogen) in progression of liver disease: guilt by association? *Semin Thromb Hemost*. 2016 June; 42(4): 397-407
37. Pawlinski R, Pedersen B, Schaubbauer G, Tencati M, Holscher T, Boisvert W, Andrade-Gordon P, Frank RD, Mackman N. Role of tissue factor and protease-activated receptors in a mouse model of endotoxemia. *Blood*. 15 February 2004; 103(4): 1342-1347
38. Foley JH, Conway EM. Cross talk pathways between coagulation and inflammation. *Circ Res*. 2016 March; 118: 1312-1408
39. Pretorius E, Bester J, Paige MJ, Kell DB. The potential of LPS-binding protein to reverse amyloid formation in plasma fibrin of individuals with Alzheimer-type dementia. *Front Aging Neurosci*. 2018 August 22; 10:257
40. Northup PG, Sundaram V, Fallon MB, Reddy KR, Balogun RA, Sanyal AJ, Anstee QM, Hoffman MR, Ikura Y, Caldwell SH. Hypercoagulation and thrombophilia in liver disease. *J Thromb Haemost*. 2008; 6: 2-9
41. Bester J, Soma P, Kell DB, Pretorius E. Viscoelastic and ultrastructural characteristics of whole blood and plasma in Alzheimer-type dementia, and the possible role of bacterial lipopolysaccharides (LPS). *Oncotarget*. 2015 October 10;
42. Kell DB, Pretorius E. The simultaneous occurrence of both hypercoagulability and hypofibrinolysis in blood and serum during systemic inflammation, and the roles of iron and fibrin(ogen). *Integr Biol*. 2014 October 13
43. Pretorius E, Mbotwe S, Bester J, Robinson CJ, Kell DB. Acute induction of anomalous and amyloidgenic blood clotting by molecular amplification of highly substoichiometric levels of bacterial lipopolysaccharide. *J R Soc Interface*. 2016 August 16; 13:20160539

44. Bitto N, Liguori E, La Mura V. Coagulation, microenvironment and liver fibrosis. *Cells*. 2018 July 24; 7(85)
45. Hong Zheng, Aimin Cai, Qi Shu, Yan Niu, Pengtao Xu, Chen Li, Li Lin & Hongchang Gao. Tissue-specific metabolomics analysis identifies the liver as a major organ of metabolic disorders in amyloid precursor protein/presenilin 1 mice of Alzheimer's disease. *J Proteome Res*. 2019; 18: 1218-1227
46. Maarouf CL, Walker JE, Sue LI, Dugger BN, Beach TG & Serrano GE. Impaired hepatic amyloid-beta degradation in Alzheimer's disease.
47. Estrada LD, Ahumada P, Cabrera D & Arab JP. Liver dysfunction as a novel player in Alzheimer's progression: looking outside the brain. *Frontiers in Aging Science*. 2019; 11(174)
48. The Rat Grimace Scale. National Centre for the Replacement, Refine & Reduction of Animal in Research. Published 01 September 2015 (last updated 11 October 2021).
49. Wahl D, Coogan SCP, Solon-Biet SM, de Cabo R, Haran JB, Raubenheimer D, et al. Cognitive and behavioral evaluation of nutritional interventions in rodent models of brain aging and dementia. *Clinical Interventions in Aging*. 8 September 2017; 12: p.1419-1428
50. Prieur EAK, Jadavji NM. Assessing spatial working memory using the spontaneous alternation Y-maze test in aged male mice. *Bio-protocol*. 5 February 2019; 9(3): p.1-10
51. Venter C. An *in ovo* investigation of the cellular effects of the heavy metals cadmium and chromium alone and in combination [dissertation]. Pretoria (GP): University of Pretoria; 2014.
52. Puzzo D, Lee L, Palmeri A, Calabrese G & Arancio O. Behavioral assays with mouse models of Alzheimer's disease: practical considerations and guidelines. *Biochem Pharmacol*. 15 April 2014; 88(4): 450-467
53. Miedel CJ, Patton JM, Miedel AN, Miedel ES & Levenson JM. Assessment of spontaneous alternation, novel object recognition and limb claspings in transgenic mouse models of Amyloid- β and Tau neuropathology. *J Vis Exp*. 28 May 2017; 123: e55523
54. Vorhees CV & Williams MT. Assessing spatial learning and memory in rodents. *ILAR Journal*. 2014; 55(2): 310-332
55. Yarube IU, Ayo JO, Magaji RA, Umar IA, Yusuf NW, Alhassan AW, Saleh MIA. Outcome of sub-acute insulin administration on long-term visuospatial and short-term working memory in mice. *J. Afr. Ass. Physiol. Sci*. July 2016; 4 (1): 41-47

56. Kim YT, Yi YJ, Kim MY, Bu Y, Jin ZH, Choi H, Dore S & Kim H. Neuroprotection and enhancement of spatial memory by herbal mixture HT008-1 in rat global brain ischemia model. *Am. J. Clin. Med.* 2008; 36: 287-299
57. Sarnyai Z, Sibille EL, Pavlides C, Fenster RJ, McEwen BS & Tóth M. Impaired hippocampal-dependent learning and functional abnormalities in the hippocampus in mice lacking serotonin_{1A} receptors. *Proc. Nat. Acad. Sci.* December 19 2000; 97: 14731- 14736
58. Rogers AB, Dintzis, RZ. Hepatobiliary System. In: Treutlers PM, Dintzis SM, Montiine KS, eds. *Comparative Anatomy and Histology: A Mouse, Rat and Human Atlas*. 2nd ed. London: Elsevier Inc; 2018. p.229-239
59. Krishna M. Microscopic anatomy of the liver. *Clinical Liver Disease*. 29 March 2013; 2(S1): S4-S7
60. Bataller R, Brenner DA. Liver fibrosis. *J Clin Invest.* 2005; 115(2): 209-218
61. Safer A, Afzal M, Hanafy, N, Mousa, S. Green tea extract therapy diminishes hepatic fibrosis mediated by dual exposure to carbon tetrachloride and ethanol: A histopathological study. *Experimental and Therapeutic Medicine*. 2015; 9(3): 787-794
62. Fang H, Liu A, Chen X, Cheng W, Dirsch O & Dahmen U. The severity of LPS induced inflammatory injury is negatively associated with the functional liver mass after LPS injection in rat model. *Journal of Inflammation*. 2018; 15(21)
63. Marzano C, Cazals-Hatem D, Rautou P-E & Valla D-C. The significance of nonobstructive sinusoidal dilatation of the liver: impaired portal perfusion or inflammatory reaction syndrome. *Hepatology*. 2015; 62: 956- 963
64. Dirchwolf M & Ruf AE. Role of systemic inflammation in cirrhosis: From pathogenesis to prognosis. *World J Hepatol.* 2015 Aug 8; 7(16): 1974-1981
65. Nürnberger S, Miller I, Duvigneau JC, Kavanagh ET, Gupta S, Hartl RT, Hori O, Gesselbauer B, Samali A, Kungl A, Redl H, Kozlov AV. Impairment of endoplasmic reticulum in liver as an early consequence of the systemic inflammatory response in rats. *Am J Physiol Gastrointest Liver Physiol.* 2012; 303: G1373-G1383
66. Schwarz DC, Blower MD. The endoplasmic reticulum: structure, function and response to cellular signaling. *Cell Mol Life Sci.* 2016; 73: 79-94
67. Ozcan L, Tabas I. Role of endoplasmic reticulum stress in metabolic disease and other disorders. *Annual Review of Medicine*. February 2012; 63: 317-328
68. Cheng Ji, Kaplowitz N. ER stress: can the liver cope? *Journal of Hepatology*. 2006; 45: 321-333
69. Zheng K, Kaufman RJ. From endoplasmic-reticulum stress to the inflammatory response. *Nature*. July 24 2008; 454(7203): 455-462

70. Khan Z, Stolz DB, Crawford JM. Ultrastructure of the hepatocyte. In: Benhamou JP, Blei A, Dufour J-F, Ginès P, Friedmann S, Reichen J, Rodes J, Valla C, Zoulim F, eds. *Oxford Textbook of Clinical Hepatology: from Basic Science to Clinical Practice*. 3rd ed. New York: Oxford University Press; 2007. pp. 20-28
71. Kozlov A, Duvigneau JC, Miller I, Nurnberger S, Gesslbauer B, Kungl A, Ohlinger W, Hartl RT, Gille L, Staniek K, Gregor W, Haindl S & Redl H. Endotoxin causes functional endoplasmic reticulum failure, possibly mediated by mitochondria. *Biochimica et Biophysica Acta*. March 25 2009; 1792: 521-530
72. Orrego H, Medline A, Blendis LM, Rankin JG & Kreaden DA. Collagenisation of the Disse space in alcoholic liver disease. *Gut*. 1979; 20: 673-679
73. Lotowska JM, Sobaniec-Lotowska ME, Lebensztejn DM, Daniluk U, Sobaniec P, Sendrowski K, Daniluk J, Reszec J & Debek W. Ultrastructural characteristics of rat hepatic oval cells and their intercellular contacts in the model of biliary fibrosis: new insights into experimental liver fibrogenesis. *Gastroenterology Research and Practice*. July 9 2017; 9 pp.
74. Mackman N. The role of tissue factor and factor VIIa in hemostasis. *Anesth Analg*. May 2009; 108(5): 1447-1452
75. Gerrits AJ, Koeman CA, Yildirim C, Nieuwland R, Akkerman JWN. Insulin inhibits tissue factor expression in monocytes. *Journal of Thrombosis and Haemostasis*. 2009; 7: 198-205
76. Rautou P.E, Tatsumi K, Antoniak S, Owen AP, Sparkenbaugh E, Holle LA, Wolberg AS, Kopec AK, Pawlinski R, Luyendyk JP, Mackman N. Hepatocyte tissue factor contributes to the hypercoagulable state in a mouse model of chronic liver injury. *J Hepatol*. Jan 2016; 64(1): 53-59
77. Sullivan BP, Kopec AK, Joshi N, Cline H, Brown JA, Bishop SC, Kassel KM, Rockwell C, Mackman N, Luyendyk JP. Hepatocyte tissue factor activates the coagulation cascade in mice. *Blood*. 2013; 121 (10): 1868–1874.
78. Kopec AK, Luyendyk JP. Coagulation in liver toxicity and disease: Role of hepatocyte tissue factor. *Thromb Res*. May 2014; 133(1): S57-S59
79. Jenne CN, Kubes P. Immune surveillance by the liver. *Nature Immunology*. October 2013; 14(10): 996-1006
80. Luyendyk JP, Maddox JF, Green CD, Ganey PE, Roth RA. Role of hepatic fibrin in idiosyncratic-like liver injury from lipopolysaccharide-ranitidine coexposure in rats. *Hepatology*. 2004; 40(6): 1342-1351
81. Neubauer K, Knittel T, Armsburst T, Ramadori G. Accumulation and cellular localization of fibrinogen/fibrin during short-term and long-term rat liver injury. *Gastroenterology*. 1995; 108: 1124-1135

82. Lee DC, Rizer J, Selenica M-LB, Reid P, Clara Kraft C, Johnson A, Blair L, N Gordon MN, Dickey CA & Morgan D. LPS- induced inflammation exacerbates phospho-tau pathology in rTg4510 mice. *Journal of Neuroinflammation*. 2010; 7(56)